Detecting Biomarkers of OCD Through the Use of Behavioral Tasks: Pilot Data Analysis and Task Validation

By

William Luke Acuff

B.S., Mississippi State University, 2020

Thesis

Submitted in partial fulfillment of the requirements for the Degree of Master of Science in the Graduate Program of Biomedical Engineering at Brown University

PROVIDENCE, RHODE ISLAND

MAY 2022

AUTHORIZATION TO LEND AND REPRODUCE THE THESIS

As the sole author of this thesis, I authorize Brown University to lend it to other institutions for the purpose of scholarly research.

Date 4/27/22 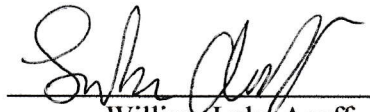

William Luke Acuff, Author

I further authorize Brown University to reproduce this thesis by photocopying or other means, in total or in part, at the request of other institutions or individuals for the purpose of scholarly research.

Date 4/27/22 

William Luke Acuff, Author

This thesis by W. Luke Acuff is accepted in its present form by the Center of Biomedical Engineering as satisfying the thesis requirement for the degree of Master of Science.

Recommended to the Graduate Council

Date 4/27/22 Signature: _____

Dr. Nicole McLaughlin, Advisor

Date 4/27/2022 Signature: _____

Dr. David Borton, Reader

Date 4/27/22 Signature: _____

Dr. Matthew Harrison, Reader

Approved by the Graduate Council

Date 4/27/22 Signature: _____

Dr. Marissa Gray, Biomedical Engineering Master's Program Director

Vita

Luke Acuff was born in Nashville and raised in Columbia, Tennessee. He attended Mississippi State University as an undergraduate, graduating *Collegiate Honorum* and *Summa Cum Laude* with a bachelor's degree in biomedical engineering and a minor in computer science. At Mississippi State, Luke performed undergraduate toxicology research under the direction of Dr. Janice Chambers, where he supported the development of novel, brain-penetrating antidotes to combat organophosphate poisoning. After graduation, Luke began the master's program in biomedical engineering at Brown University where he developed and taught the course *Engineering Biomedical Systems* for the Summer@Brown program and joined the lab of Dr. Nicole McLaughlin. Alongside members of the McLaughlin lab and the lab of Dr. David Borton, Luke developed and executed the PROVOC project at Butler Hospital as part of a wider NIH UH3 grant to improve Deep Brain Stimulation as treatment for intractable Obsessive-Compulsive Disorder.

Preface and Acknowledgments

Data for the PROVOC project were collected in the TMS Clinic at Butler Hospital. Participant eligibility was screened with assistance from Rebecca Poncin, Hasan Raza, Anna Sherman, and Yunshu Fan, and participants were psychiatrically assessed by Nicole McLaughlin and Anna Sherman. Behavioral and electrophysiological data were collected alongside Yunshu Fan. The original Conveyor Belt Provocation Task was designed by Nicole Provenza, Nicole McLaughlin, Eric Storch, Wayne Goodman, and Evan Matteson, and associated hardware was built by Evan Matteson. Hardware was updated with assistance from Sam Parker and Nicole Provenza, and the task protocol was updated alongside Yunshu Fan and Anna Sherman. The original Computer Provocation Task was designed by Nicole Provenza, Nicole McLaughlin, Eric Storch, and Wayne Goodman and was programmed by Fernando Gelin and Mary McGrath. The task and code were updated alongside Ivo Su and Yunshu Fan. Funding for project PROVOC comes from NIH Grant 5UH3NS100549-03.

I would also like to acknowledge the innumerable, unnamed sources of input who contributed over the course of this multi-institution, multi-year project. I would additionally like to acknowledge the current and future research participants whose contribution made and will make this research possible. Personally, I would like to thank Dr. Nicole McLaughlin for bringing me into her lab and both Dr. McLaughlin and Dr. David Borton for their guidance and assistance in bringing this project to life. I would like to further thank Dr. McLaughlin, Dr. Borton, and Dr. Matthew Harrison for providing their input and expertise in the writing of this thesis. I would like to thank Frances Kronenberg and Dr. Yunshu Fan for their input on EEG analysis, and I would especially like to thank Dr. Fan for her constant mentorship, support, and collaboration in all aspects of project PROVOC, without which this research would not have been possible. Finally, I would like to thank my family and friends for their support over the course of my development at Brown.

Table of Contents

Table of Figures

Table of Tables

Chapter 1: Introduction

Obsessive-compulsive disorder (OCD) is a neuropsychiatric disorder affecting an estimated 1.6-2.3%[1,2] of the general population characterized by unwanted thoughts (obsessions) and repetitive behaviors (compulsions) which significantly disrupt an individual's daily life. Obsessions are repetitive, persistent, and unwanted thoughts, ideas, or urges which distress an individual to the point of engaging in neutralizing or suppressive behaviors. These behaviors, called compulsions, are repetitive mental or physical acts which feel as though they must be performed, as they provide temporary relief from OCD-induced distress, a related feeling of 'completeness,' or are seemingly performed automatically.[3–5] The behavioral relationship between obsessions and compulsions is thought to be cyclical; performing compulsions reinforces obsessive fears and reliance on the compulsions themselves to an extent that is often deemed excessive and irrational even by the individual performing them.[4,6] Psychological distress as a resultant and driver of the disorder is then critical to the behavioral and neurological motivations which enable the disease, and the induction of obsessive-compulsive (OC) distress could be used to isolate neural activity related to the disorder. Detecting neural mechanisms, or biomarkers, which lead to OC distress is also critical to advancing treatment of the disorder, as neuromodulation therapies such as adaptive deep brain stimulation (aDBS) could be tailored to modulate brain regions responsible for OCD in real time.

Features, Subtypes, and Symptoms of OCD

OCD is a largely heterogeneous disorder, and as such can present in a variety of different ways with variable obsessions, compulsions, and relationships between the individual and their symptoms. Obsessions commonly consist of concerns about contamination, harm to oneself or others, sexual or violent thoughts or urges, or symmetry, but are not limited to these examples and can present in practically any form imaginable. Compulsions commonly include excessive cleaning, checking, prayer, thought control, ordering, and counting.[5–8] OCD should also be differentiated

from other psychiatric disorders despite sharing similar traits.[3,4] Unlike specific phobias, obsessions demand extreme importance in an individual's life outside of direct exposure to the offending stimulus, often manifesting as time-consuming threats to one's well being necessitating extensive rumination, compulsion performance, and/or painstaking avoidance strategies. Furthermore, worries and rumination brought about by generalized anxiety disorder (GAD) and major depressive disorder (MDD) are less ego-dystonic and typically have more rational, real-world themes than OCD obsessions, and are rarely accompanied by compulsions.[3,9]

Due to the extreme heterogeneity of OCD, multi-dimensional models of the disorder are used to group distinct features of OCD together into symptom subtypes. Exploratory dichotomous factor analysis using individual OCD symptoms as defined by the Yale-Brown Obsessive Compulsive Scale[10] identified five subtypes: symmetry/ordering, hoarding, contamination/cleaning, doubt/checking, and taboo thoughts.[11] Of note, since the release of the DSM-V, the hoarding subtype has been redefined as hoarding disorder (HD) and reclassified as one of the obsessive-compulsive and related disorders.[4] Another multi-dimensional model of OCD defines only two subtypes distinguished by OC motivation: harm avoidance and incompleteness.[7]

Individuals with OCD also tend towards a series of common neurocognitive defects, with studies showing deficits in executive functioning, working memory, and attention being especially common.[12,13] Underlying psychological factors, or 'core features' of OCD across subtypes which may lead to these traits include abnormal risk assessment, pathological doubt, and incompleteness.[8]

Neuroanatomical Model of OCD

Neurological factors are thought to significantly contribute to OCD, as neuroimaging studies have shown discrepant brain activity between individuals with OCD and healthy controls.[3,13–15] In particular, the orbitofrontal cortex (OFC), anterior cingulate cortex (ACC), and limbic system have shown higher levels of activity in OCD, especially during provocation. These hyperactivities are shown to decrease after successful treatment using either selective serotonin reuptake inhibitors (SSRIs) or cognitive-behavioral therapy (CBT), further implicating OFC, ACC, and the limbic

system in the neuropathology of OCD.[13–15] Whether this hyperactivity drives OCD symptoms or results from them is still debated. However, acquired OCD and OCD-like symptoms are correlated with lesions to the basal ganglia and cerebral cortex in humans and animals,[16,17] strengthening the hypothesis that abnormal activity in these regions contributes to OCD.

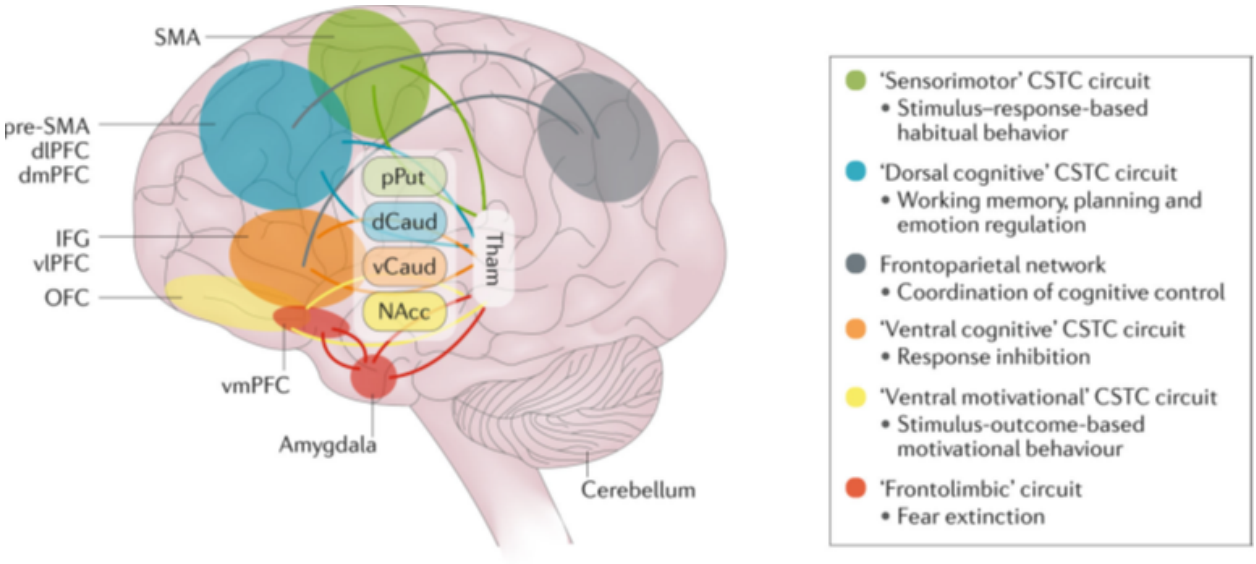

Figure 1: CSTC Circuits in OCD. Adapted from Stein et al.[3]

OCD-relevant brain regions are hypothesized to coordinate through parallel, cortico-striato-thalamo-cortical (CSTC) neural circuits, or corticostriatal pathways. As seen in Figure 1, these circuits describe connectivity between cortical regions and the limbic system, forming loops which mediate sensorimotor, cognitive, affective, and motivational processes.[18–20] CSTC circuits are further conceptualized as being composed of direct and indirect projection pathways across cortical and limbic regions to modulate thalamic and cortical activation; as seen in an example CSTC circuit in Figure 2, direct pathways form a positive feedback loop and disinhibit the thalamus, while indirect pathways balance the direct as a negative feedback loop inhibiting the thalamus.[14]

Dysfunction, or imbalance, between direct and indirect pathways in OCD-implicated CSTC circuits by overactivity of the direct pathway relative to the indirect could lead to various deficits which would explain symptoms of OCD. Proposed deficits induced by this imbalance in implicated CSTC circuits include impaired response inhibition and the inability to transition from ha-

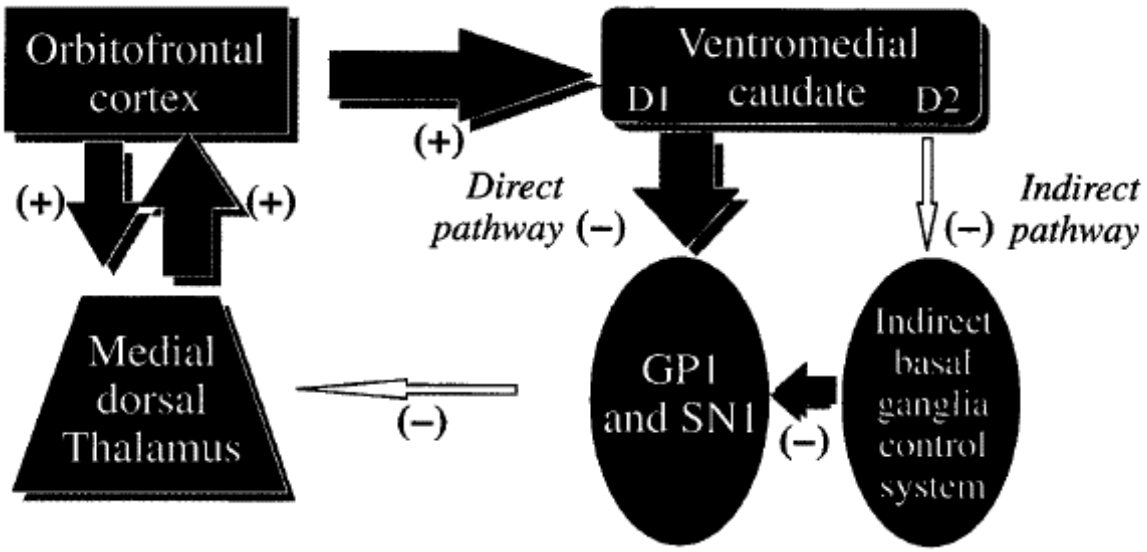

Figure 2: Model of a Direct and Indirect Pathway for CSTC Pathophysiology in OCD. Adapted from Saxena and Rauch.[14]

bitual to goal-oriented behavior, contributing to compulsions, and difficulties with fear extinction, contributing to obsessions.[14,18] Successful treatment of OCD by neuroablation and deep-brain stimulation (DBS) also implicates CSTC related brain regions in contributing to OCD. Neuroablation targets shown to be beneficial in reducing symptoms of OCD include the anterior limb of the internal capsule (ALIC), the ACC, and the subcaudate region, all of which are represented in CSTC circuits.[21] DBS targets similarly involved regions, including the ventral striatum (VS), ALIC, the subthalamic nucleus (STN), caudate nucleus (CN), and the inferior thalamic peduncle (ITP).[21–23] As such, CSTC circuit dysfunction is hypothesized to be one of the primary neurological factors driving OCD.

Treatment, Deep Brain Stimulation, and the Need for Biomarkers

Standard first-line treatment options for OCD are psychotherapy, pharmacotherapy, or a combination of both.[24] However, relapse in symptoms following partial remission is still reported in approximately half of OCD patients receiving behavioral therapy and pharmacological treatment, making the need for more effective treatment clear.[24,25] Supplemental to psychotherapy and pharmacotherapy for treatment-resistance cases of OCD are neuromodulation and ablative neuro-

surgery techniques.[21,26] Neuromodulation can be further subdivided into transcranial direct current stimulation (tDCS), repetitive transcranial magnetic stimulation (rTMS), and DBS, with DBS reaching an impressive 60% response rate in largely treatment-resistant individuals.[23] However, DBS has considerable stimulation related side-effects and requires invasive neurosurgery which comes with its own risks.[21] And with 40% of individuals unresponsive, there is clearly still room for improvement.

DBS for treatment of OCD is thought to disrupt pathological corticostriatal pathways by delivering adjustable stimulation via implanted depth electrodes to deep-brain areas such as ALIC, VS, STN, ITP, and CN.[22,27,28] The mechanisms for this disruption aren't well understood, but consideration of the immediate and delayed effects of DBS for OCD suggests that DBS acts via several distinct mechanisms. Leading hypotheses suggest that short term therapeutic effects (improvement of mood and anxiety) result from immediate modulation of pathological neural circuits, while long term effects (reduction in OCD symptoms) are mediated by synaptic plasticity and eventual anatomical remodeling. However, as symptoms of OCD often return when stimulation is discontinued, permanent modulation of pathological pathways (the short term effect) may be necessary to keep pathological CSTC activity from overriding long-term anatomical changes.

Given the functional similarity to neuroablation therapy in both target and effect, DBS was initially thought to act as a functional, reversible lesion by inhibiting neurons near the point of stimulation.[28] Conversely, new evidence suggests that DBS might increase neuronal firing, but in a manner than disrupts time-variable information travelling through the stimulated region, maintaining the 'functional lesion' effect without inhibition.[28] Some theorists suggest that the effects of DBS are better understood not as a loss of information, but as forcing neuronal information to reorganize in a way that improves symptoms of the pathology in question without 'disabling' the region at all.[28] Despite this uncertainty, DBS is still known to be effective in treating OCD. However, further exploration of the exact mechanisms of DBS and the neurocircuitry it acts on will be necessary to optimize the therapy moving forward.

Current DBS for OCD treatment paradigms have two major drawbacks, stimulation-related side effects and the inconsistent nature of OCD symptoms. There is no ideal DBS stimulation level; the system must be tuned to the individual to adequately address symptoms while avoiding side-effects. The primary side-effect of DBS is hypomania, which is attenuated by reducing DBS stimulation amplitude.[29] This is typically done by a physician who changes the settings on an ad-hoc basis. This tuning is delicate, however, as stimulation amplitude being set too low could provide insufficient relief of OCD symptoms, and the effects of a new stimulation level are not immediately obvious, making repeat visits necessary if symptoms change. Furthermore, this tuning happens over days or weeks, while OCD symptoms can vary drastically on their own over much shorter timeframes. An adaptive DBS (aDBS) system could address this by detecting hypomanic or obsessive-compulsive episodes and appropriately adjusting stimulation parameters. However, an 'obsessive-compulsive episode' represents a complex cognitive state which, as of now, cannot be reliably detected by neural recording alone. To this end, a deeper understanding of relevant neural activity in the brain as it experiences obsessive-compulsive symptoms is necessary to make recommendations for future aDBS detection technology.

Obtaining Biomarkers with Electroencephalography (EEG)

aDBS systems would likely rely on intracranial electrocorticographic (ECoG) or deep-brain depth electrodes to assess neural activity in OCD patients. However, the risks and expense of neuro-surgery, in addition to the small number of patients with implanted DBS devices keep large scale exploratory DBS electrode placement from being feasible. Electroencephalography (EEG), on the other-hand, is a relatively cheap, easy, and safe method to assess neural activity on a larger scale.

EEG is a neural recording methodology which uses electrodes placed on the scalp to detect changes in surface potential.[30] Those slight changes are mostly indecipherable to the naked eye, but when amplified and converted to a digital format, they can be analysed and compared across subjects, tasks, and conditions to highlight relevant deviations in cortical activity.

Quantitative EEG (qEEG) is an EEG methodology used to quantify continuous EEG waveforms

with signal processing techniques such as the Fast Fourier Transform and Welch's Method to generate human-interpretable data.[31] This process devolves a finite, continuous signal such as the recorded voltage at a scalp electrode during a particular task into its component frequencies to generate a frequency spectrum. Taken together, these spectra are thought to partially reflect brain activity and are commonly used to further quantify psychiatric disorders.[32,33] However, inter-trial and inter-participant variance make studies with repetitive task performance and large sample sizes necessary to effectively separate irrelevant neurological 'noise' from relevant neurological 'signal' by assuming that irrelevant signals will eventually average out but that salient, pathological activity will remain mostly constant. Furthermore, in order to effectively interpret frequency spectra, the processed signal is typically broken down into historically pre-defined bands of frequency thought to represent distinct types of activity.[34] Commonly these are defined as Delta (1-4 Hz), Theta (4-8 Hz), Alpha (8-15 Hz), Beta (15-30 Hz), and Gamma (30+ Hz), though even these ranges are not stringently defined across literature.

EEG's primary drawback is depth; scalp electrodes cannot reliably portray activity in deep brain areas such as the thalamus and wider limbic system which as previously mentioned are thought to be integral to the pathophysiology of OCD. Despite this, EEG can portray activity in cortex, meaning OCD-critical areas such as OFC and ACC could meaningfully contribute to EEG signal. Therefore, large scale EEG data collection with the goal of capturing and quantifying OCD brain activity could guide future aDBS electrode placement and the development of a closed-loop aDBS algorithm.

Locating Biomarkers of OCD Through the Use of Behavioral Tasks: Project PROVOC

Project PROVOC is an experimental protocol designed to locate biomarkers of OCD by monitoring the neural activity of individuals with OCD, specific phobia (SP), and healthy controls as they perform behavioral tasks meant to induce symptoms of OCD, phobia, or general distress. The PROVOC procedure has been in development at Brown University and Butler Hospital since 2017, with the eventual goal of providing data to be used in directing future aDBS research concerning

the detection of OC cognitive states in real time.

PROVOC consists of four behavioral tasks: the Conveyor Belt Provocation Task (Conveyor Belt PROVOC, or CBP), the Computer Provocation Task (Computer PROVOC, or CpP), the Multi-Source Interference Task (MSIT), and the Beads Task. PROVOC has three phases, a clinical assessment phase to validate participant cohort placement, an in-clinic phase to collect neurological and other electrophysiological data during each of the four behavioral tasks, and a virtual, longitudinal data collection phase to assess the effects of attenuation on repeated performances of the MSIT, Beads, and Computer PROVOC tasks. In this study, pilot provocation task (Conveyor Belt PROVOC and Computer PROVOC) data gathered from one participant during the in-clinic phase is analysed to validate the protocol for future use.

Chapter 2: Data Collection Methods

Electrophysiological Monitoring Setup and In-Clinic Procedure

Participants for the study are recruited from the general population and divided into three cohorts: healthy controls with no history of psychiatric diagnosis, specific phobia participants, and OCD participants. Participants are screened by trained clinicians to confirm cohort placement before arriving at Butler Hospital for the in-clinic phase of the study. Electrophysiological data are collected using the BrainVision actiCHAMP Plus System.[35] Once in-clinic, participants are fitted with a 64-channel BrainVision EEG actiCAP device, galvanic skin resistance (GSR) monitor, electrocardiogram (ECG), and horizontal electrooculogram (HEOG).

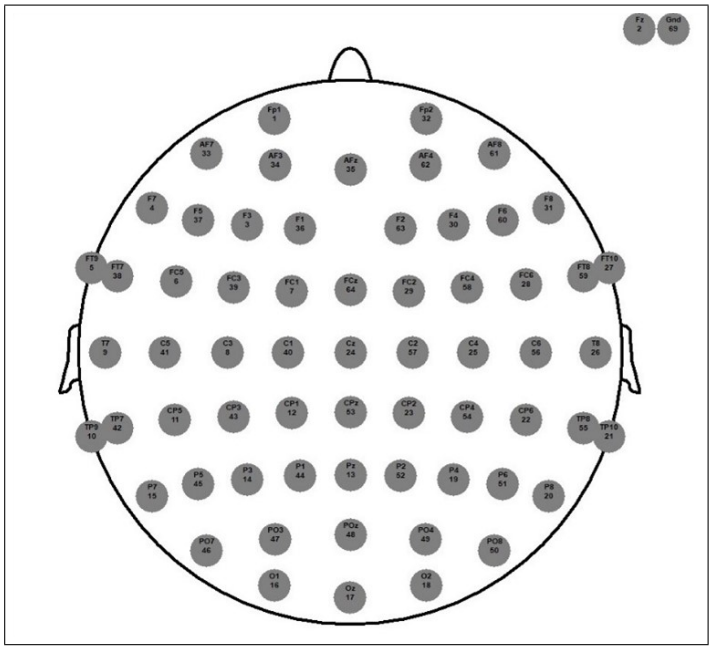

Figure 3: BrainVision 64-channel EEG montage.[35,36]

The BrainVision EEG actiCAP houses 64 active Ag/AgCl (sinter) surface electrodes (Fp1, Fz, F3, F7, FT9, FC5, FC1, C3, T7, TP9, CP5, CP1, Pz, P3, P7, O1, Oz, O2, P4, P8, TP10, CP6, CP2, Cz, C4, T8, FT10, FC6, FC2, F4, F8, Fp2, AF7, AF3, Afz, F1, F5, FT7, FC3, C1, C5, TP7, CP3, P1, P5, PO7, PO3, Poz, PO4, PO8, P6, P2, CPz, CP4, TP8, C6, C2, FC4, FT8, F6, AF8, AF4, F2, FCz) positioned according to the BrainVision 64-channel EEG montage – based on the international 10-10 electrode system – as depicted in Figure 3. EEG, GSR, ECG, and HEOG signals are sampled at 1 kHz, amplified by the BrainVision actiCHAMP amplifier system, and recorded by the BrainVision Recorder software.[36] Relevant experimental signals from

Conveyor Belt PROVOC, Computer PROVOC, MSIT, and Beads are captured by the BrainVision Triggerbox and recorded by BrainVision Recorder.

Virtual tasks (Resting State, MSIT, Beads, and Computer PROVOC) are performed on a Windows Surface Pro tablet. Participants begin with a resting state task to establish baseline EEG, GSR, ECG, and HEOG recordings. Participants then complete the MSIT task, Beads task, Computer PROVOC task, an additional resting state task, and finally the Conveyor Belt PROVOC task, concluding the in-clinic phase of the study.

Computer PROVOC (CpP) Task

Before the in-clinic phase, 10 non-distressing (neutral) and 10 distressing (provoking) images are chosen by the research team and tailored to the participant for use in the Computer PROVOC task. A set of 10 generic, calm, environmental images are used for all cohorts as neutral images. Healthy control participants are assigned distressing images from the International Affective Picture System (IAPS)[37] database. Specific Phobia and OCD participants are assigned distressing images individually tailored to trigger phobic or OCD distress.

(a) Image Exposure **(b)** SUDS Rating

Figure 4: Computer PROVOC Task Visualization

In-clinic, the Computer PROVOC Task consists of a one-trial non-distressing training block followed by 2 main blocks with 60 trials each. Each trial consists of one image drawn from the pool of combined distressing and non-distressing images assigned to the participant, flashing onto the screen for 2.5 seconds before being replaced by a wheel of numbers ranging from 0 to 10. The participant selects the number which best represents their Subjective Units of Distress Scale (SUDS)

rating for the image they just saw. After SUDS rating selection, the next trial begins. Over the course of the entire task, each individual image is displayed 6 times, for a total of 60 neutral trials and 60 provoking trials. Participants are guided through a deep breathing exercise between the 1st and 2nd block.

Conveyor Belt PROVOC (CBP) Task

The Conveyor Belt PROVOC task is designed to expose participants to *in vivo* triggers that are considered by the participant to elicit their OC or phobic symptoms.

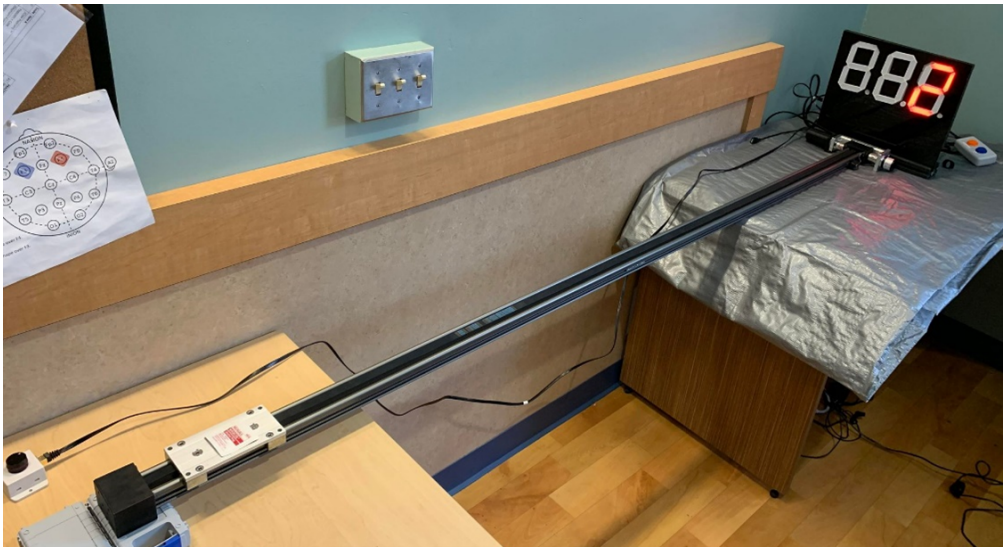

Figure 5: Conveyor Belt PROVOC setup with caddy extended to Position 5 (closest to the participant). Hand dial is used to enter SUDS ratings, which are shown on the display.

Before the task, the research team selects three objects per participant, 1 non-distressing and 2 designed to trigger distress. OCD or phobic distressing objects are tailored to the participant's specific OCD or phobic triggers. Objects are chosen to evoke general distress for healthy controls. The conveyor belt caddy moves between 5 different positions, with position 1 being furthest from the participant at approximately 230 cm away, position 2 at 180 cm, position 3 at 130 cm, position 4 at 70, and position 5 being closest at approximately 20 cm from the participant.

At the start of the task, the object is revealed on the caddy at Position 1, signaling the start of the first rating period and first block, during which the object is stationary. During this and all

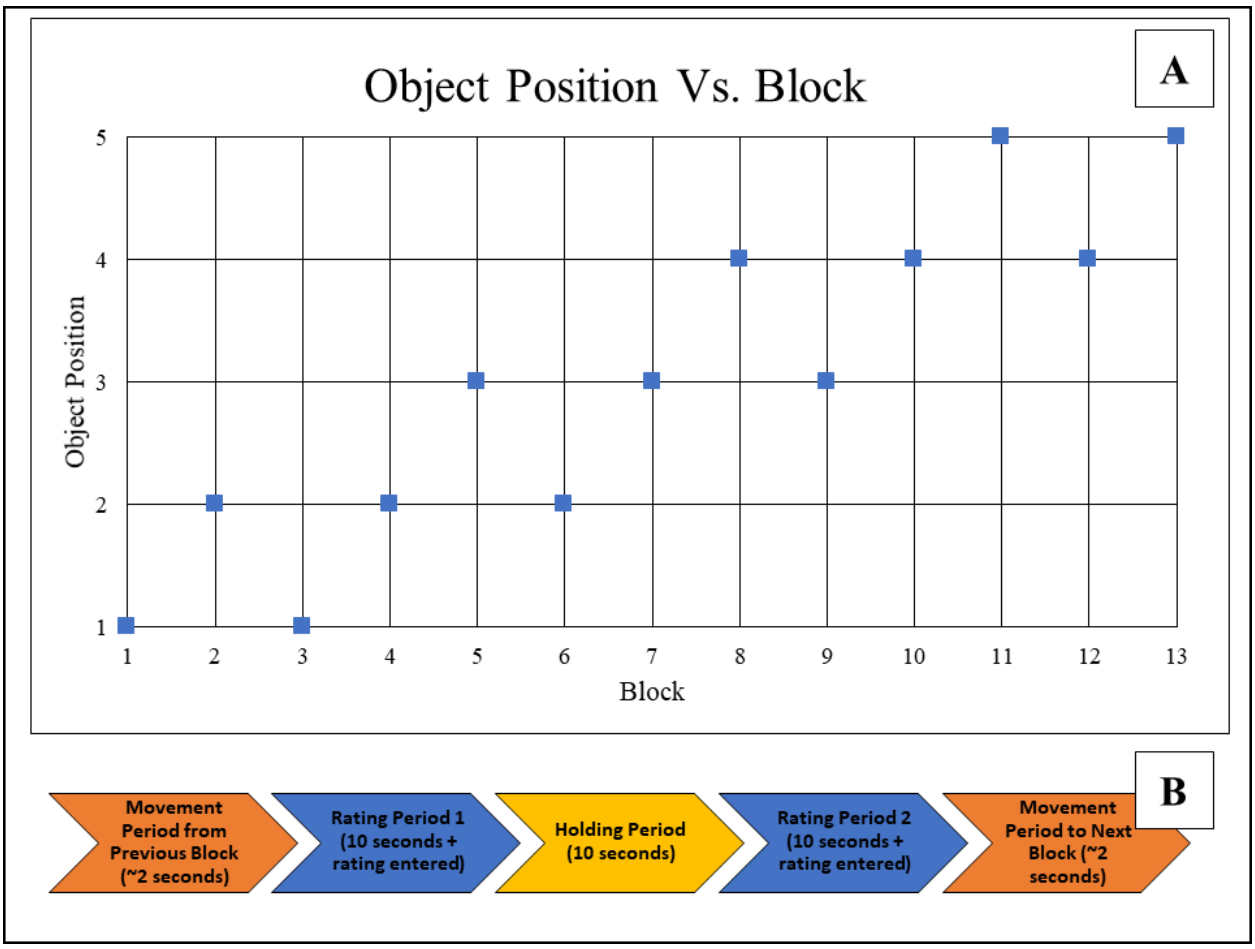

Figure 6: Conveyor Belt PROVOC Task Visual Timeline. Part A: Object Position Vs. Block, where Position 1 is furthest from the participant and Position 5 is closest to the participant. Part B: Description of a single block.

rating periods, the participant is prompted to submit a SUDS rating; once ten seconds are up and a rating has been submitted, the rating period ends. After the initial rating period the object remains stationary without any SUDS input for an additional ten seconds during what is referred to as the holding period. At the end of the holding period, the second rating period begins. At the end of this rating period, the first block (consisting of a rating period followed by holding period followed by another rating period, as shown in Figure 5b) ends, and the conveyor belt moves the object forward to the next block's position over a period of approximately two seconds in what is referred to as the movement period. Then, a new rating period begins, starting the next block.

Research Subject

Due to an initial delay caused by the COVID-19 pandemic and subsequent protocol modifications, equipment issues, shipping delays, and personnel changes, the first participant (referred to as BH_301) completed his in-person visit for project PROVOC on March 18th, 2022, years past the project's originally anticipated data collection phase and still months past the COVID-adjusted timeline. For the purposes of this analysis, only those data collected during BH_301's in-person visit are considered.

BH_301 is a 27 year old male diagnosed with OCD in 2018. His self-reported obsessions primarily concern mercury, asbestos, and radiation contamination, with accompanying compulsions of frequent and intense hand-washing and avoidance of potentially contaminated objects, people, or locations. His respective scores for relevant OCD assessments are listed in Table 1, including the Yale-Brown Obsessive Compulsive Scale (YBOCS),[10] the Yale-Brown Obsessive Compulsive Scale II (YBOCS II),[38] the Obsessive-Compulsive Inventory (OCI),[39] and the Sheehan Disability Scale (SDS).[40]

Assessment	**Indication**	**Range**	**Score**
YBOCS	OCD Symptom Severity	0-40	28
YBOCS II	OCD Symptom Severity	0-50	33
OCI	Level of OCD Distress	0-72	27
SDS	Level of Disability	0-30	20

Table 1: OCD Assessments

While the specific significance of these scores are beyond the scope of this analysis, they generally indicate moderate to severe OCD. Furthermore, BH_301's contamination obsession includes several everyday objects, making symptom provocation safe and feasible.

For the Computer PROVOC task, 10 provoking images were selected from an internet search: 2 asbestos themed, 4 radiation themed, and 4 mercury themed. As seen in Figure 7 for the Conveyor Belt PROVOC task, a innocuous plastic card holder was chosen as the non-provoking control and a CFL mercury containing light bulb and loose insulation were chosen as provoking objects.

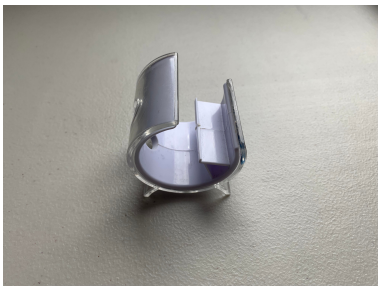

(a) Control (Non-Provoking) CBP Object: Plastic Card Holder

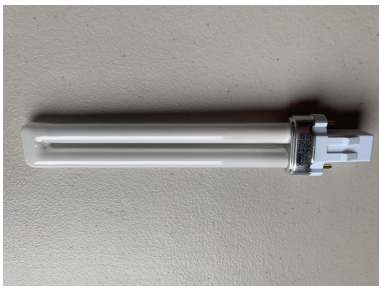

(b) Provoking CBP Object 1: CFL Mercury Lightbulb

(c) Provoking CBP Object 2 - Loose Insulation

Figure 7: Conveyor Belt PROVOC Provocation Props

During the in-person visit, the GSR electrodes failed to make good contact with the participant's skin, necessitating skin-conductivity's exclusion from this analysis. ECG electrodes placed on the participant's chest also failed to make good contact, but were switched to the participant's wrists in time to get good recordings for the second resting-state and Conveyor Belt PROVOC tasks.

Chapter 3: Data Preprocessing Methods

The BrainVision actiCHamp suite samples data from 64 actiCAP scalp electrodes and other auxiliary electrodes at 1 kHz, generating gigabytes of data per recording. However, before any meaningful analysis can happen, these data must be trimmed, cleaned, and organized in a uniform way across tasks and participants.

Task Synchronization

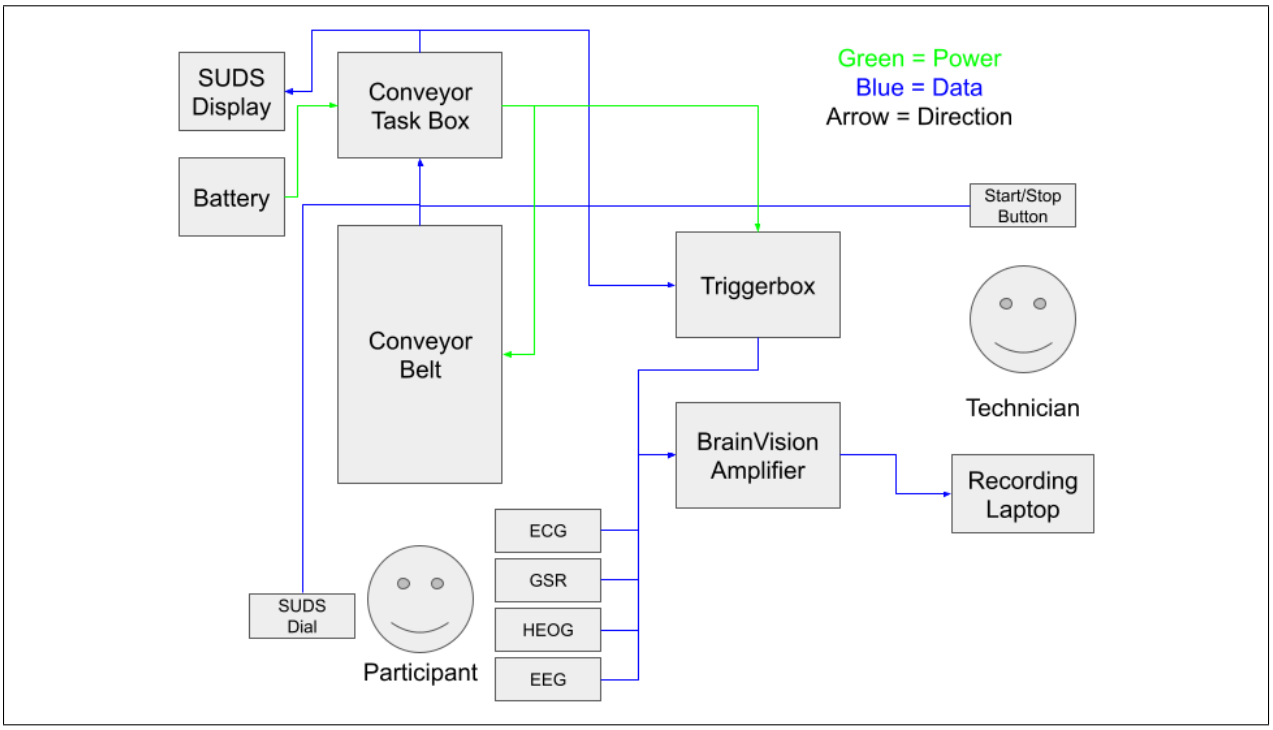

Figure 8: Conveyor Belt PROVOC Task Data/Power Flowchart

For this study, all data – electrophysiological and task – must be accurately recorded and time-synced for later analyses to be accurate. The BrainVision actiCHamp suite records ECG, GSR, and HEOG alongside EEG data; however, data such as the score and timing of SUDS ratings (responses) and the type and timing of provocation (stimuli) during each task must be recorded externally and fed into the BrainVision system as it records in the form of event markers. This necessitates the use of the Triggerbox, a BrainVision hardware extension which accepts wired

serial or parallel digital inputs, interprets them, and feeds them into the actiCHamp suite as it records.

During Computer PROVOC, relevant stimulus and response event markers are generated by provided Brainvision software in concert with the Computer PROVOC executable program. These markers travel from the task computer to the Triggerbox's serial port via a USB cable. During Conveyor Belt PROVOC, this process is considerably more complicated. As visualized in Figure 8, the conveyor belt itself and other task implements are controlled by a central Conveyor Task Box containing a micro-controller (Arduino Uno) programmed with instructions to move the belt back and forth (Figures 5, 6), interpret the SUDS dial, and update the SUDS display.

Binary Output	**Interpreted Code**	**Code Indication**
0001	S1	Dial to Pos. 1
0010	S2	Dial to Pos. 2
0011	S3	Dial to Pos. 3
0100	S4	Dial to Pos. 4
0101	S5	Dial to Pos. 5
0110	S6	Dial to Pos. 6
0111	S7	Dial to Pos. 7
1000	S8	Dial to Pos. 8
1001	S9	Dial to Pos. 9
1010	S10	Dial to Pos. 10
1011	S11	Dial to Pos. 0
1100	S12	SUDS Submitted
1101	S13	Rating Period Begins
1111	S15	Emergency Stop
001	R1	Conveyor to Pos. 1
010	R2	Conveyor to Pos. 2
011	R3	Conveyor to Pos. 3
100	R4	Conveyor to Pos. 4
101	R5	Conveyor to Pos. 5
110	R6	Holding Period Begins
111	R7	Trial Ends

Table 2: Conveyor Belt PROVOC Event Codes: 4 bit binary outputs represent S codes on bits 0-3, while 3 bit binary outputs represent R codes on bits 4-6.

The task hardware was initially designed to send task information to the since-replaced Open Ephys[41] EEG system; as such, compatibility updates were necessary for BrainVision. Without

Arduino compatible BrainVision software, the Triggerbox serial port used for Computer PROVOC was abandoned in favor of the simpler, on-board parallel communication port. Experimentation revealed that the Triggerbox parallel port used an edge detector to register new event markers, taking the binary value of the parallel bits as the event code once a change is detected. As such, 8 new leads (bits 0-6 and ground) were soldered onto the Arduino, which had its code updated to reset the voltage (Low: Digital Zero - 0 Volts | High: Digital One - 5 Volts) of its new outbound leads corresponding to Table 2. To account for rare instances in which two event markers would be sent at once – such as the SUDS button being pressed (S12), which could immediately initiate a new holding period (R6) – event markers were split into S and R codes, traditionally used to distinguish between stimuli and responses but in this case to designate bits 0-3 to an initial set of events and bits 4-6 to the remaining set of events which might overlap with the first.

With updated software and hardware, event markers for both provocation tasks are stored in proper time alongside all electrophysiological data recorded by the BrainVision actiCHamp suite. Matlab scripts using the open source EEGLAB[42] plugin further process these events as the first EEG preprocessing step, labeling them with proper trial names, participant IDs, and other necessary information not explicitly contained in the event codes themselves to make downstream analysis smoother.

EEG Downsampling, Filtering, and Artifact Subspace Reconstruction

Once event markers are properly synced and labeled, EEG data are loaded into EEGLAB and downsampled from 1000 Hz to 250 Hz to reduce file size and increase computational speed. While this lowers the data's Nyquist Frequency (Sampling Rate/2) to 125 Hz, the maximum frequency under analysis is 45 Hz, meaning that signal of interest is safe from unintentional aliasing. EEG data are then high-pass filtered with a digital FIR filter at 1 Hz to remove baseline drift (Figure 9).

Next, using the EEGLAB Clean Rawdata function, channels with high frequency noise over 4 standard deviations from the mean and flat channels are removed. Clean Rawdata then uses the Artifact Subspace Reconstruction[43] (ASR) algorithm to identify and correct high-variance artifacts

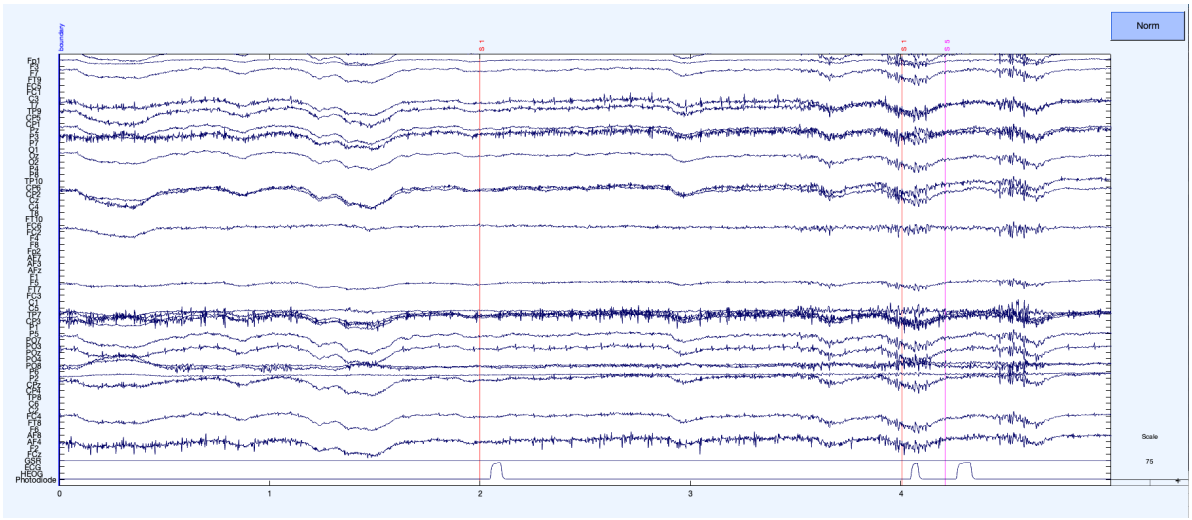

(a) Raw EEG Data before Preprocessing

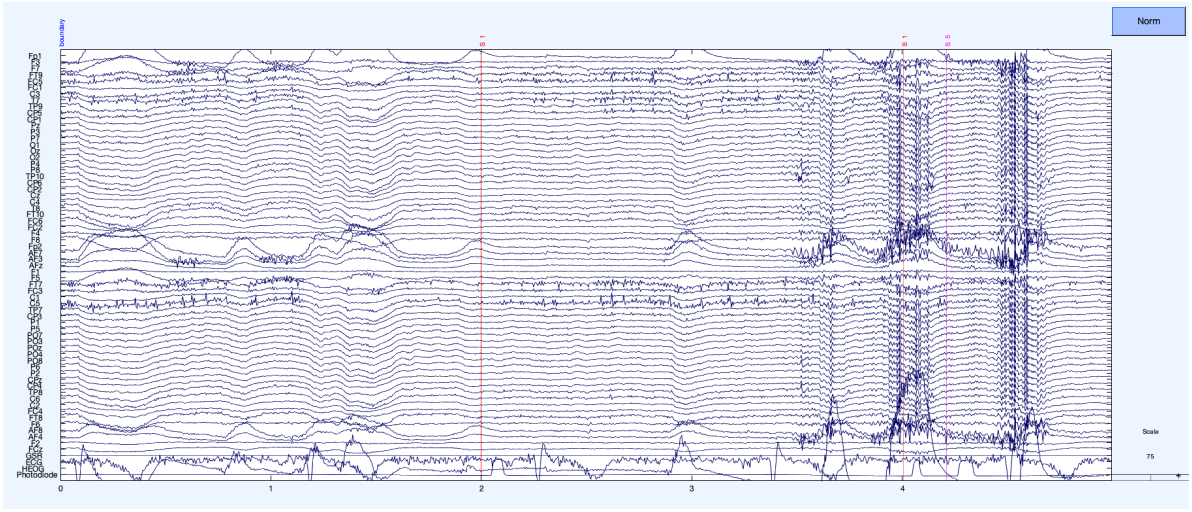

(b) Downsampled to 250 Hz and HPF at 1 HZ

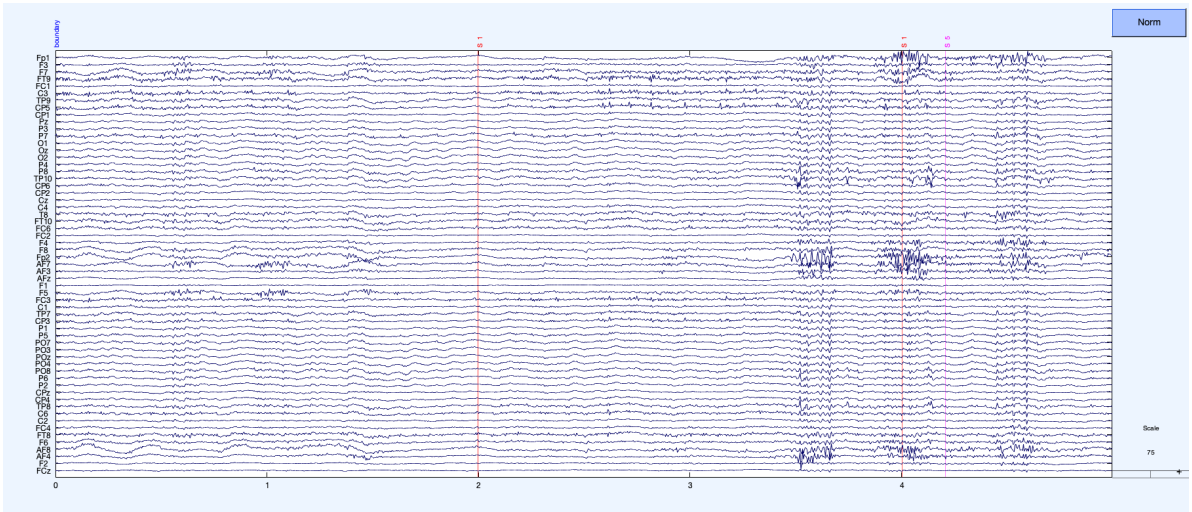

(c) Cleaned with Artifact Subspace Reconstruction

Figure 9: EEG Preprocessing - Downsampling, Filtering, and Artifact Subspace Reconstruction (Viewed in EEGLAB)

as defined by exceeding the cutoff threshold, k, of 20 standard deviations in a 0.5 second window. This method provides powerful artifact correction, but its effect on underlying brain signal are not entirely understood.[44] However, the excess of electromyographic (EMG) noise thought to have been generated by the participant's facial tics during provocation tasks necessitated aggressive artifact removal in order to preserve enough data for analysis. The online reference channel (Fz) and any removed channels are then interpolated and returned to the data before re-referencing each channel to average.

EEG Independent Component Analysis (ICA)

Following initial preprocessing steps, Independent Component Analysis (ICA) is used to devolve EEG data into a series of topographical components (Figure 10a) which summed together represent the continuous EEG signal. Each component has topographic features corresponding to scalp location and time/frequency domain features corresponding to predicted electrophysiological activity. As seen in Figure 10b, these features can be used to identify the source of a component; localization towards the eyes, low-frequency power, and consistent, finite activity bursts all indicate Component 1 represents blink artifact. IClabel, another EEGLAB function, uses these features to label each component as brain, muscle, eye, heart, line noise, channel noise, or other with a listed percent confidence. All components labeled as eye or muscle over 80% confidence are removed from the data (Figure 10c, 10d).

EEG Epoching

Once cleaned, EEG data is cut into small segments called epochs (Figure 11) and separated into groups for further analysis. For Computer PROVOC, epochs begin at each event marker representing the onset of image exposure followed by at least 2 seconds of uninterrupted data. Epochs end after two seconds have elapsed. Event markers followed by a boundary event within 2 seconds are not considered, as boundary events indicate the deletion of data during preprocessing and would signal that the epoch is incomplete. For Conveyor Belt PROVOC, epochs are taken from holding

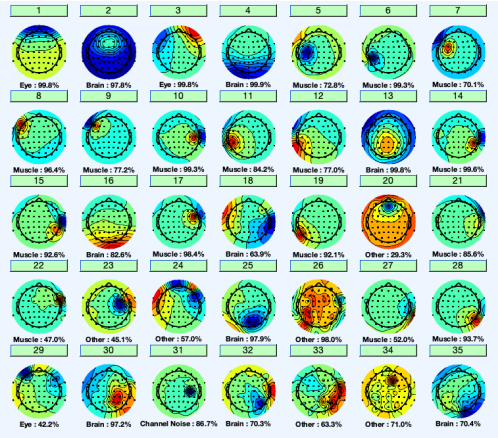

(a) All ICA Results

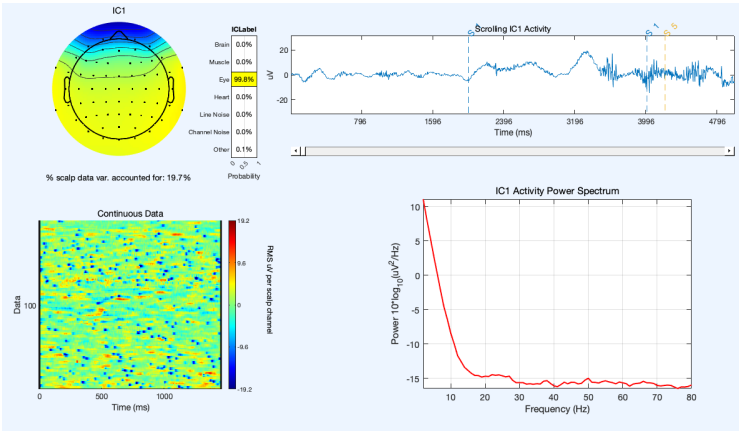

(b) Component 1 Results

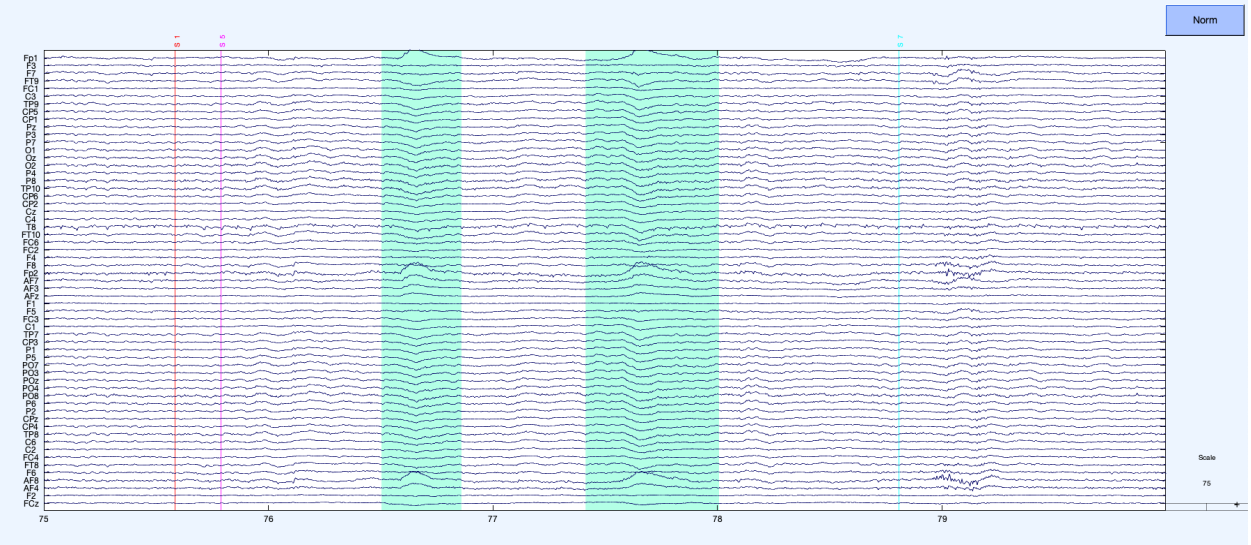

(c) Pre Artifact Component Removal (Suspected Blinks Highlighted in Green)

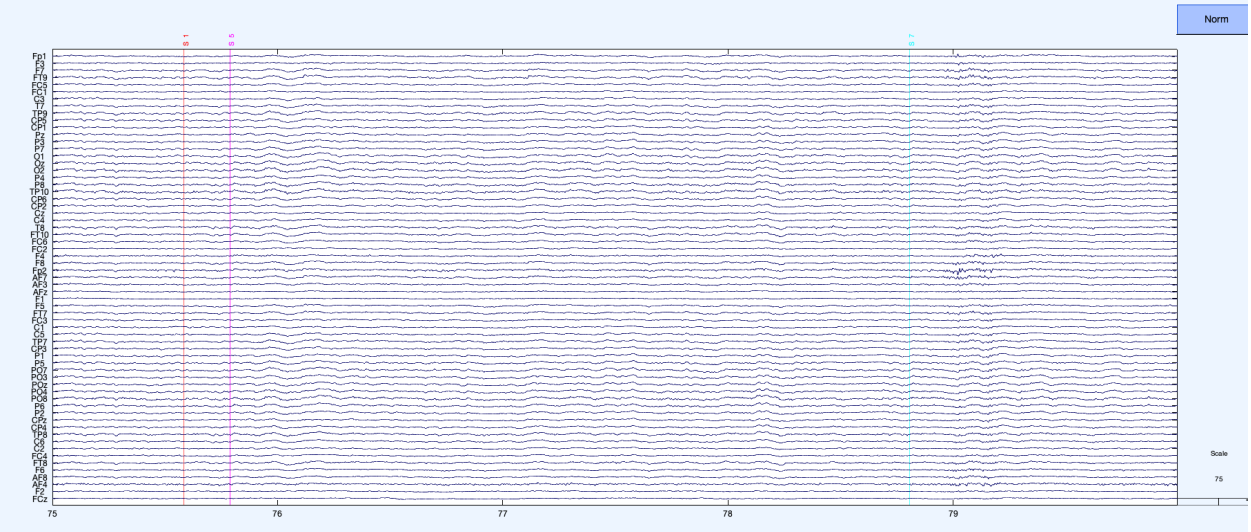

(d) Post Artifact Component Removal

Figure 10: EEG Preprocessing - Independent Component Analysis

periods (Figure 5B) as the holding period in each block is immediately preceded by a SUDS rating at the same conveyor location, the period is consistently 10 seconds long, and, unlike the rating periods, do not involve the participant performing any sort of self-reflection or muscular activity needed to submit SUDS ratings, as such reflection or muscular activity could introduce unintentional noise or bias into the data. Similar to Computer PROVOC, these epochs are 2 seconds long (5 epochs per holding period) and are not considered if they contain boundary events.

Finally, Computer PROVOC epochs are seperated into three groups: provoking epochs, during which a provoking image is shown, neutral epochs, during which a neutral image is shown, and all epochs for SUDS correlation analysis. Conveyor Belt PROVOC epochs are similarly seperated into provoking epochs, during which a provoking object is on the conveyor belt, neutral epochs, during which the control object is on the conveyor belt, and all epochs for SUDS correlation analysis.

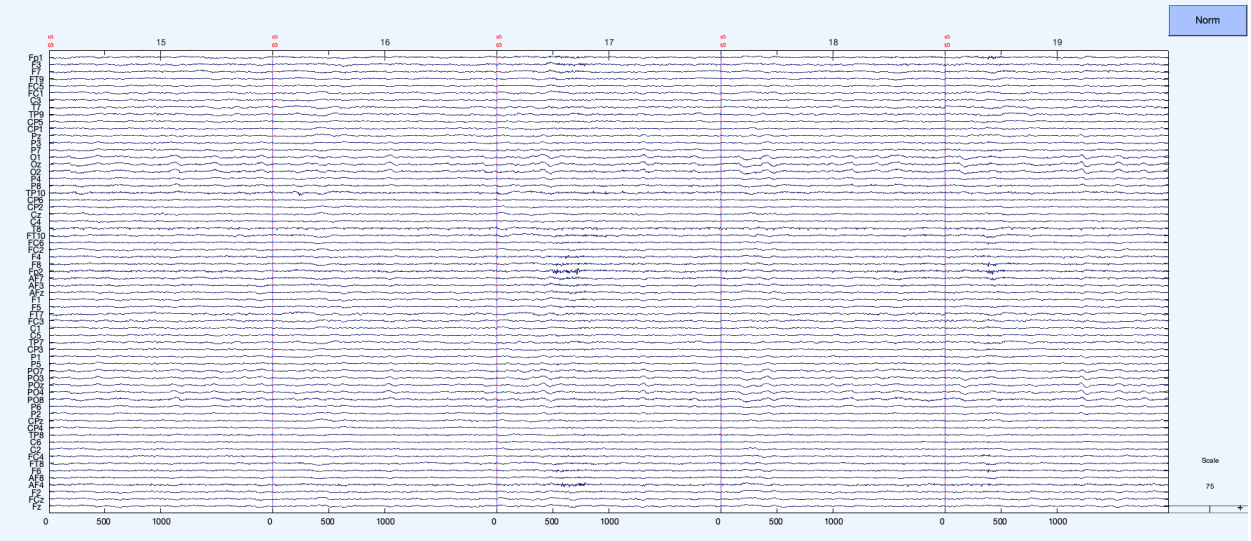

Figure 11: Fully Preprocessed, Epoched Data

ECG Preprocessing

Unlike EEG data, ECG data are measured over the span of an entire trial or task. To preprocess, ECG data are downsampled to 250 Hz and high-pass filtered at 0.5 Hz with a digital FIR filter to remove baseline drift. The data are then filtered using an 8 point moving average to improve readability and reduce the power of non-QRS signals. Using the QRS detection algorithm[45] within

the FMRIB EEGLAB plugin, QRS events are then labeled with new event markers. Finally, the data are inspected by eye to remove noisy periods and correct improperly labeled QRS events.

Once processed, QRS event markers are extracted from ECG data to generate N-N intervals. These intervals can be used to calculate Root Mean Square of Successive Differences (RMSSD) and Standard Deviation of NN Intervals (SDNN), both of which are common heart rate variance (HRV) metrics used to assess features of psychiatric conditions.[46]

Chapter 4: Behavioral/ECG Analysis

The goal of analysing non-neural data is to both quantify the level of distress the participant experienced in each task and to verify that an 'OC state' was achieved at the appropriate time. However, this is an imprecise analysis; the study does not collect perfect information about the participant's experience as the internal criteria informing participant reported distress (SUDS) is expected to vary from participant to participant and potentially from task to task. While participants are explicitly instructed to report SUDS based on how they feel in that given moment, it is entirely possible that they will let other factors, like dislike for an image or object, or even symmetry of past ratings, affect their current SUDS rating. Furthermore, precise control of a participant's level of distress is not guaranteed. Participant focus will wander from task to task, and given the sometimes sporadic nature of OCD, it is entirely possible that a neutral epoch will reflect an OC brain state during the midst of a stimulus-unrelated intrusive thought, or that a provoking epoch will reflect a non OC brain state if the participant fails to pay attention to the task at hand.

Despite these uncertainties, these tasks are designed to hold the attention of the participant as much as possible (to encourage intentional provocation), and frequent breaks are offered when appropriate to restore the participant to a baseline level of distress (to discourage unintentional provocation). Finally, both tasks include a large number of trials, 60 provoking and 60 neutral for Computer PROVOC and 2 provoking and 1 neutral (each trial containing 13 blocks and 26 ratings) for Conveyor Belt PROVOC. Besides ensuring that enough data remains after EEG preprocessing, this is also intended to improve the data's integrity if a small number of epochs do not induce the provoked or neutral state they are designed to or are not accurately represented by SUDS.

Computer PROVOC Behavioral Response

Figure 12 displays the behavioral results of the Computer PROVOC task. A clear trend is seen between provoking and neutral image trials; provoking images are consistently rated between 0 and 7 SUDS, while neutral images all received a SUDS rating of 0. This indicates that most

provoking images are producing some level of OC provocation and that neutral images are not. If SUDS ratings are further assumed to be internally consistent, it can also be assumed that the participant experienced a range of distress throughout the trial, allowing for future correlation analysis between SUDS and brain activity.

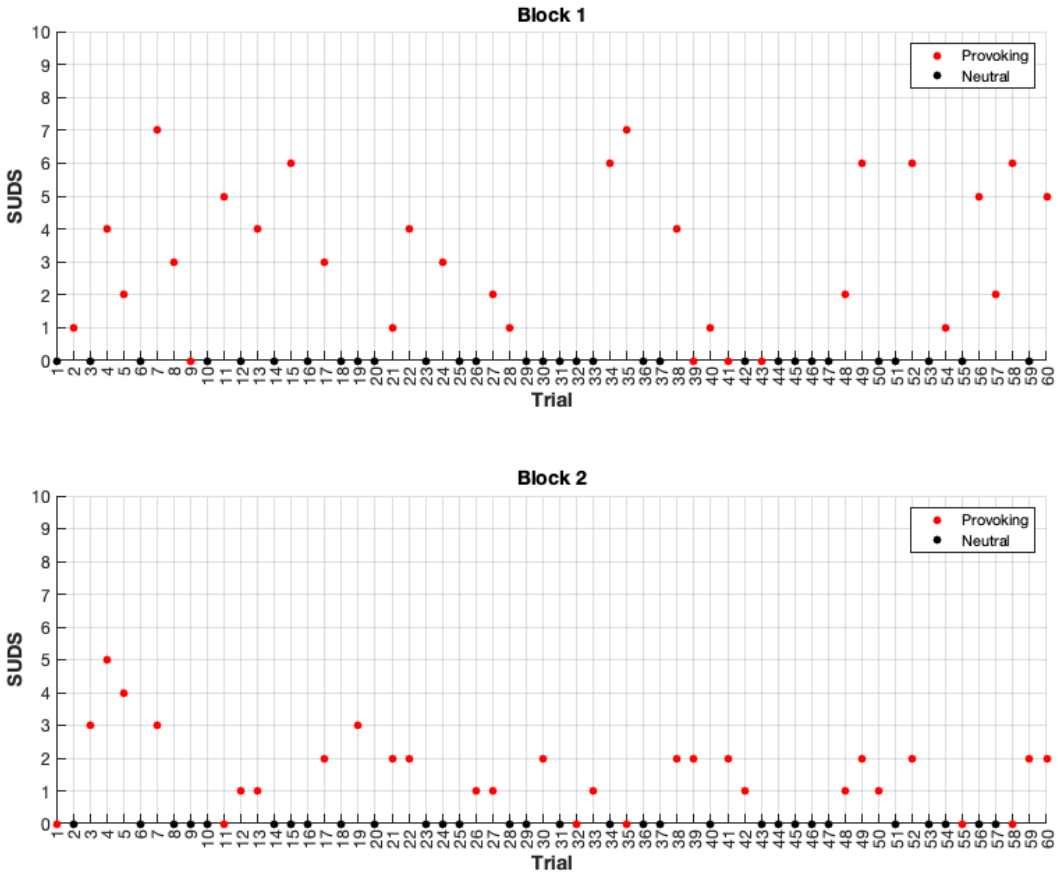

Figure 12: Computer PROVOC Behavioral Response: SUDS vs Trials

Conveyor Belt PROVOC Behavioral Response

Figure 13 and 14 display the behavioral results of the Conveyor Belt PROVOC task. In addition to the trial type and SUDS rating dimensions present in Computer PROVOC, Conveyor Belt PROVOC also offers object position, correlating to the participant's proximity to the belt object, and Nth rating, representing the order in which ratings were submitted, which corresponds to how

long the participant had been exposed to the object.

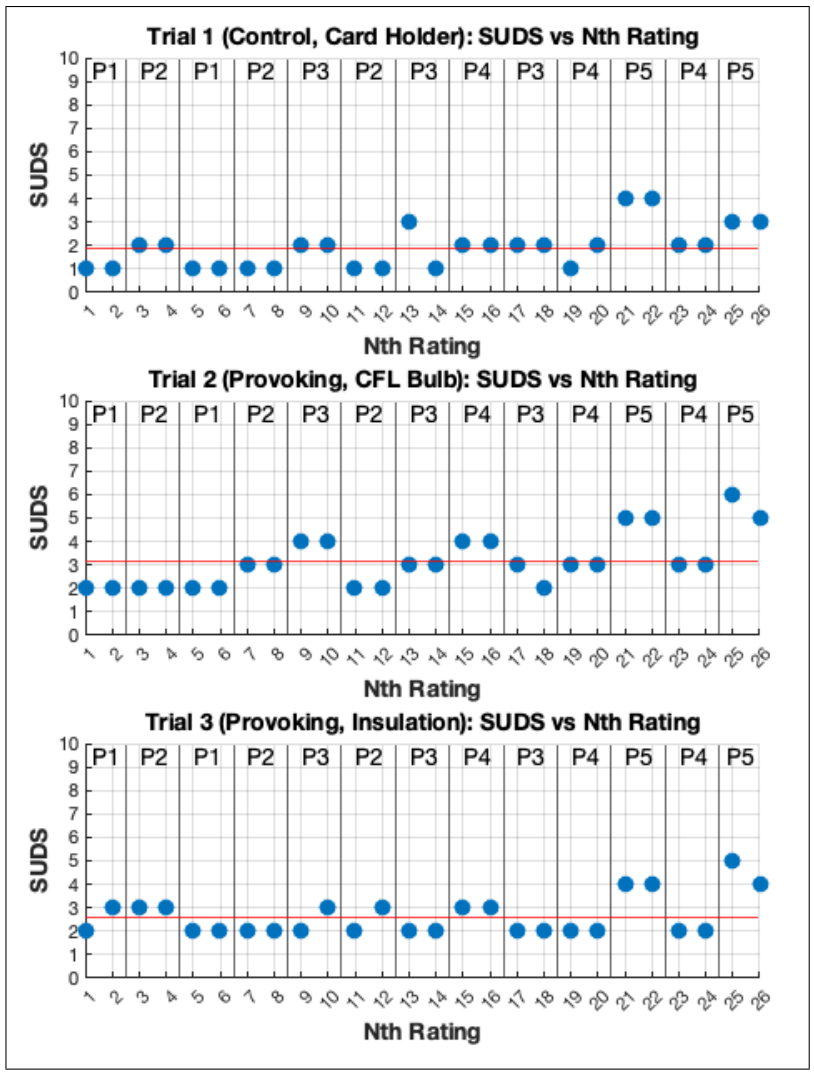

Figure 13: Conveyor Belt PROVOC Behavioral Response: SUDS vs Nth Rating. Trial Mean SUDS Visualized by Horizontal Red Line, Object Position Visualized by P1-5 Vertical Partitions.

Several conclusions can be drawn from Figure 13. First, it seems that the participant was distressed during the control trial, which used a thought-to-be neutral object on the conveyor belt. After the experiment concluded, the participant indicated that he thought the plastic card holder on the belt might be contaminated as a part of the study, causing his distress. This is unfortunate, as the lack of a proper control trial casts doubt on the validity of differences observed between 'provoking' and 'neutral' CBP trials. Nonetheless, differences between the two groups might still prove noteworthy, especially if the difference between the types of objects outweigh the participants uncertainty in terms of brain activity.

Otherwise, Figure 13 indicates that distress gradually increased over time in all three trials, again providing a range of distress for SUDS correlation analysis. It is difficult to say with certainty whether this is due to increased time spent with the object in view or increased proximity to the

object, as position and Nth rating are correlated due to the task scheme (Figure 5A). However, Figure 14 demonstrates that SUDS ratings increase with position, but SUDS rating stay constant or even decrease with Nth rating within a single position. This indicates that proximity plays a bigger role in recruiting distress than time spent exposed to the object.

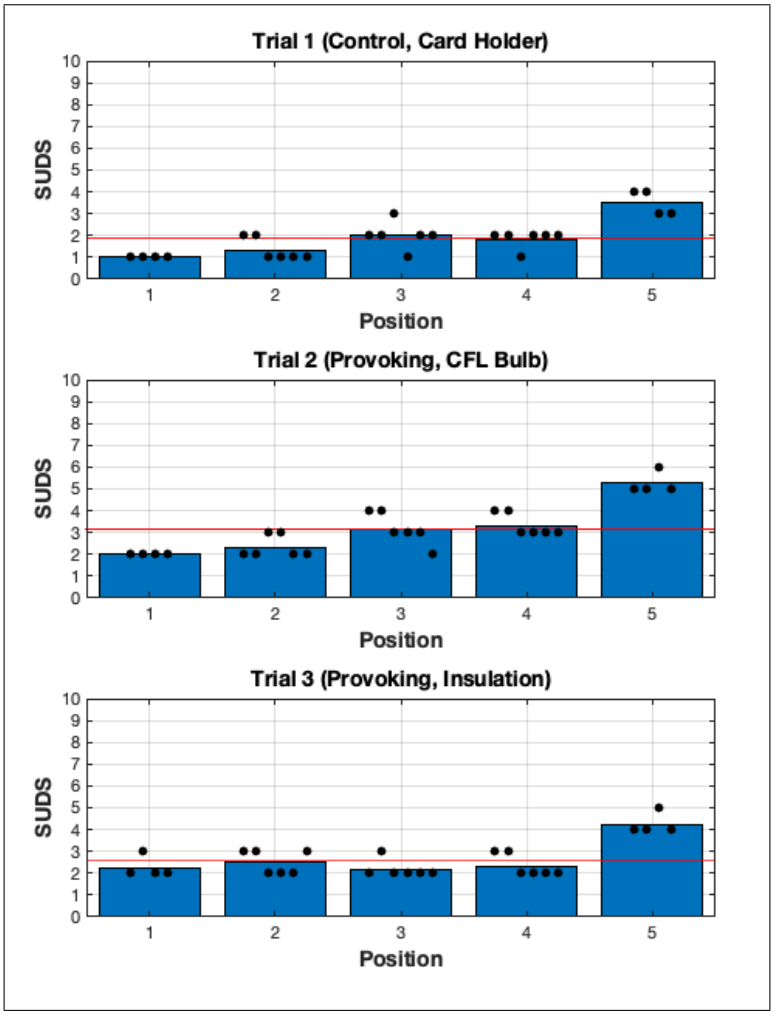

Figure 14: Conveyor Belt PROVOC Behavioral Response: SUDS vs Position. Position Mean SUDS Visualized by Blue Bars, Trial Mean SUDS Visualized by Horizontal Red Line, Nth Rating SUDS (Within Position) Visualized by Pips from Left (Earlier) to Right (Later)

Conveyor Belt PROVOC Heart Rate Variance

Figure 15 displays heart rate variance (HRV) and beats per minute (BPM) data for each of the three Conveyor Belt PROVOC trials and the 2nd resting state task: the only four recordings which generated readable ECG data. While it is good know that these data are collectable for project

PROVOC, 5 minute intervals are typically used to collect single HRV timepoints for larger comparisons.[46] Therefore, 4 HRV timepoints for 1 participant is unlikely to indicate anything useful. However, once project PROVOC has recruited and processed more participants, useful trends could emerge between cohorts.

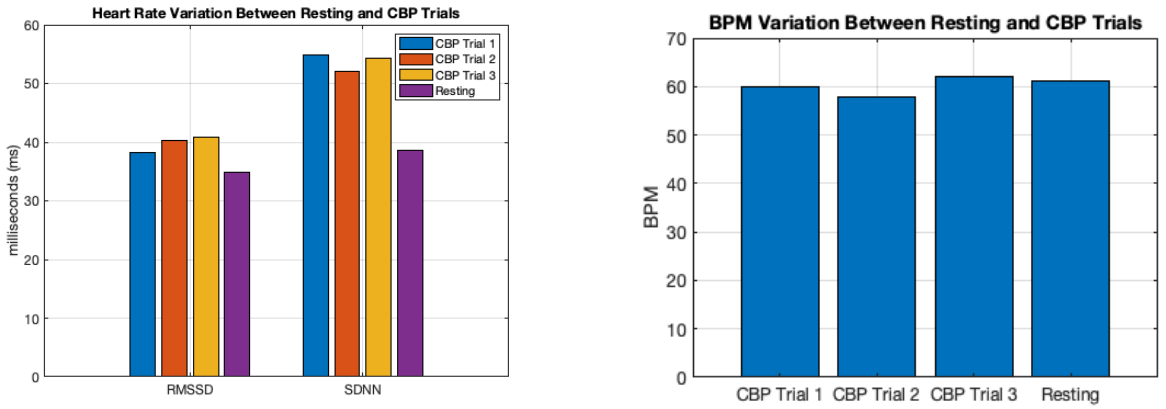

(a) Heart Rate Variance

(b) Beats Per Minute

Figure 15: Heart Rate Variance and BPM

Indications for EEG Analysis from Behavioral Result

These behavioral task data have two primary implications. The first is that the participant experienced a range of low to high distress during both Computer PROVOC and Conveyor Belt PROVOC. The second is that while Computer PROVOC provoking trials were clearly more distressing than neutral trials, the difference between provoking and neutral trials in Conveyor Belt PROVOC is less pronounced.

First, it could be assumed that brain activity during provoking trials is meaningfully distinct from neutral trials; as provoking trials scored higher SUDS than neutral trials on average in both tasks, this is a fair assumption to make. While some level of bleed-over distress might occur – such as fixating on a past provoking trial during a neutral trial – it can be further assumed that the signal difference between all averaged provoking epochs and all averaged neutral epochs would be substantial. In this case, SUDS ratings can also be ignored, keeping their potential inconsistency from biasing the results.

However, it could also be assumed that the relevant brain activity evoked during provocation is better modeled by a mathematical trend than by a binary on/off state. Rather than looking for differences between provoked and neutral states, brain activity could be quantified by how it scales with distress. In this case, 'provoking' and 'neutral' trial labels can be ignored and replaced with SUDS rating alone. If SUDS ratings are assumed to be accurate, or at least internally consistent, then this form of analysis removes uncertainty from neutral or provoking trials not achieving their desired effect, as SUDS would be the only relevant behavioral metric.

As this research is exploratory, neither assumption is known to be more accurate and both could be true, necessitating the need to do both types of analysis to see what trends emerge. A combinatorial metric using both SUDS and trial label to produce distress weights for each epoch was also considered, but ultimately not implemented to reduce the complexity of the initial analysis.

Chapter 5: EEG Analysis

As discussed in Chapter 4, EEG data are analysed in two different ways: Direct State Comparison, or looking for differences in mean activity between two distinct states, and SUDS Correlation, or looking for correlation between SUDS and activity.

In this analysis, brain activity is quantified as the Log normalized Power Spectral Density (PSD) in units of 10*$\text{Log}_{10}(\mu V^2/Hz)$, or decibels (dB) of a given frequency band: Delta (1-4 Hz), Theta (4-8 Hz), Alpha (8-15 Hz), Beta (15-30 Hz), or Gamma (30-45 Hz). While the upper end of Gamma frequency is often described as exceeding 100 Hz, the significant overlap with peak EMG noise (surface EMG frequency ranges from 10 to 1000 Hz, peaking at between 50-100 Hz[47]) and line noise (60 Hz in the US) necessitated limiting the frequency band to 45 Hz.

PSD is calculated by feeding the signal recorded at one channel during a single epoch into the EEGLAB spectopo function, which uses Welch's method[31] to devolve the signal of interest into its frequency components. For this analysis, Welch's method is set to use 250 ms Hanning Windows to best capture the signal of interest with 50% overlap between windows to preserve signal at the windows' extremes. PSD within a specified frequency range is the range's mean PSD.

PSD is further subdivided into absolute (AbsPSD) or relative (RelPSD) PSD, where AbsPSD is the PSD within the specified frequency range and RelPSD is AbsPSD of the specified frequency range divided by the AbsPSD of the entire measured frequency range (1-45 Hz).

Power Spectral Density: Direct State Comparison

Figure 16 depicts the first step in Direct State Comparison analysis, generating PSD for each channel from 1-45 Hz and averaging all epochs of a similar type within a task together.

As there are 64 recording electrodes, this method generates 64 graphs per participant per task, displayed in Appendix A for the CpP task and Appendix B for the CBP task. Table 3 contains the number of epochs per task per state for Direct State Compairson.

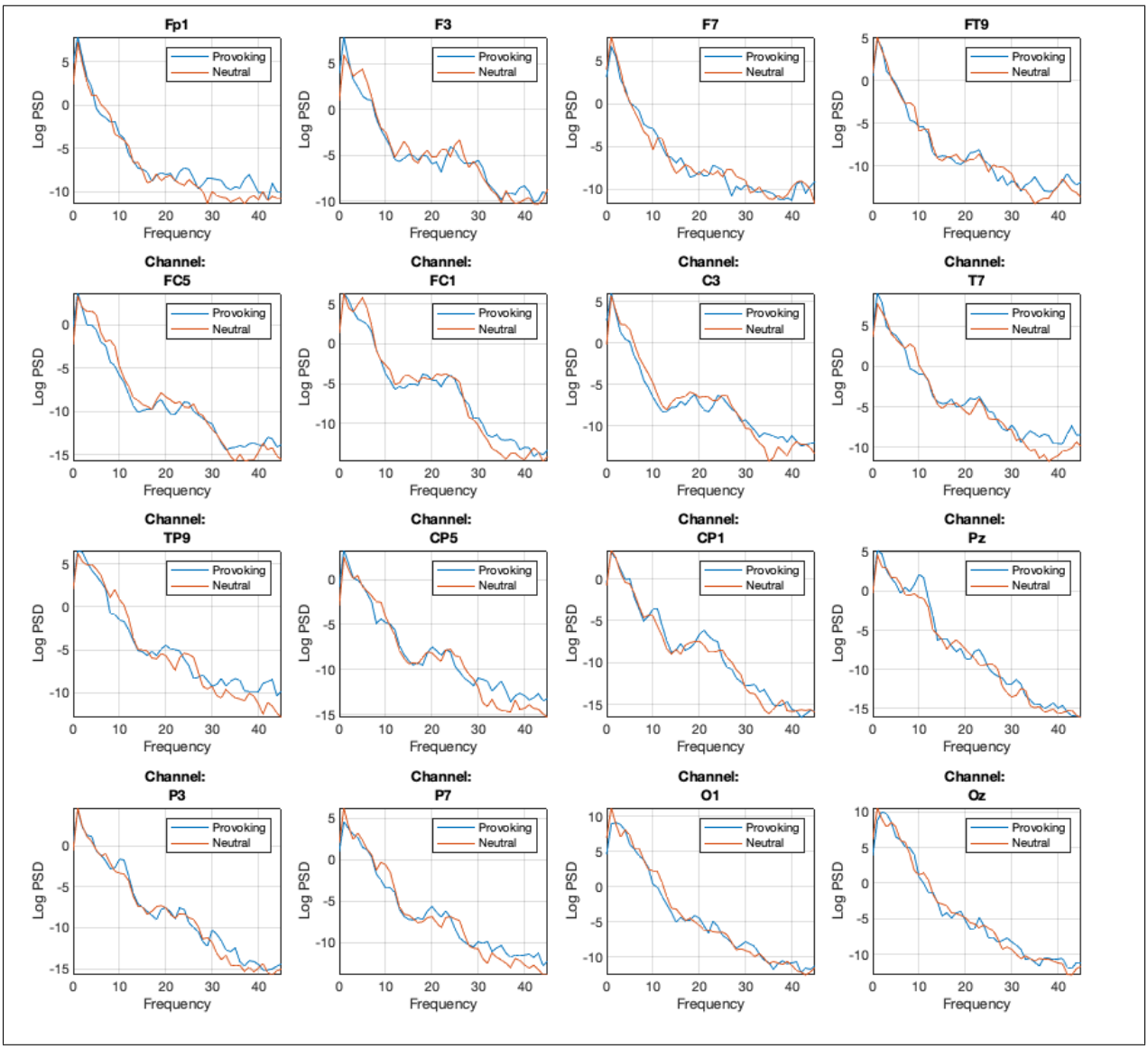

Figure 16: Select Spectra from CpP Direct State Comparison. Log PSD units in dB. Frequency units in Hz.

Task	State	Epochs
CpP	Provoking	17
CpP	Neutral	17
CBP	Provoking	60
CBP	Neutral	29

Table 3: Direct State Comparison: Epochs per Task per State

Alternatively, separating the data into blocks of frequency ranges, assuming those ranges represent distinct types of brain activity, makes the data more quantifiable. Furthermore, plotting all epochs individually on the same graph rather than averaging them all together highlights their distribution. This technique is used to generate box plots seen in Figure 17.

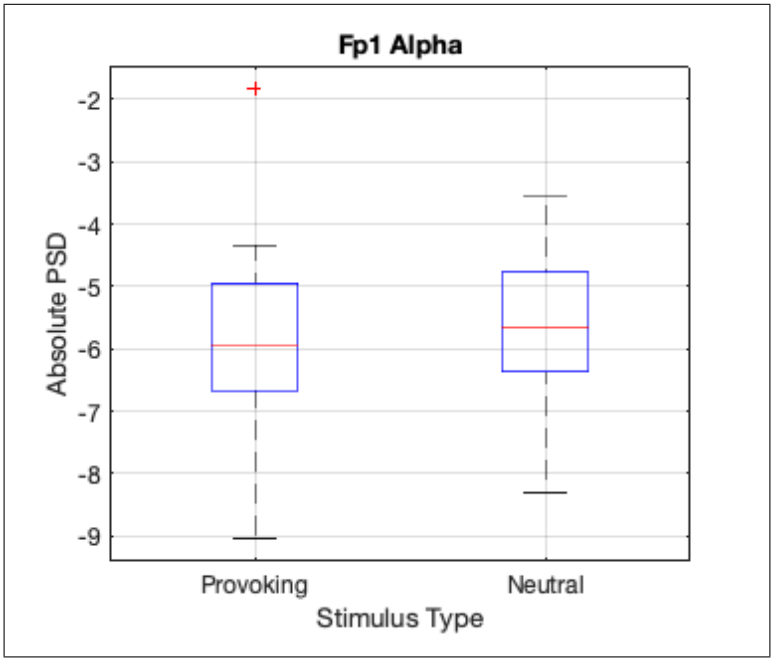

Figure 17: Direct State Comparison: Box Plot of Channel Fp1 Abs Alpha PSD during CpP. Absolute PSD units in dB.

This level of analysis provides even greater detail, but with 5 frequency bands, absolute and relative PSD, 2 tasks, and 64 channels, the resulting 1,280 box plots per participant is an indigestible amount of data. However, mean difference between states can be represented on a color spectrum, and if plotted across a topographic visualization of channel locations, data trends become visible such as in Figure 18.

While this form of visualization is much better at displaying trends, it fails to take statistical sig-

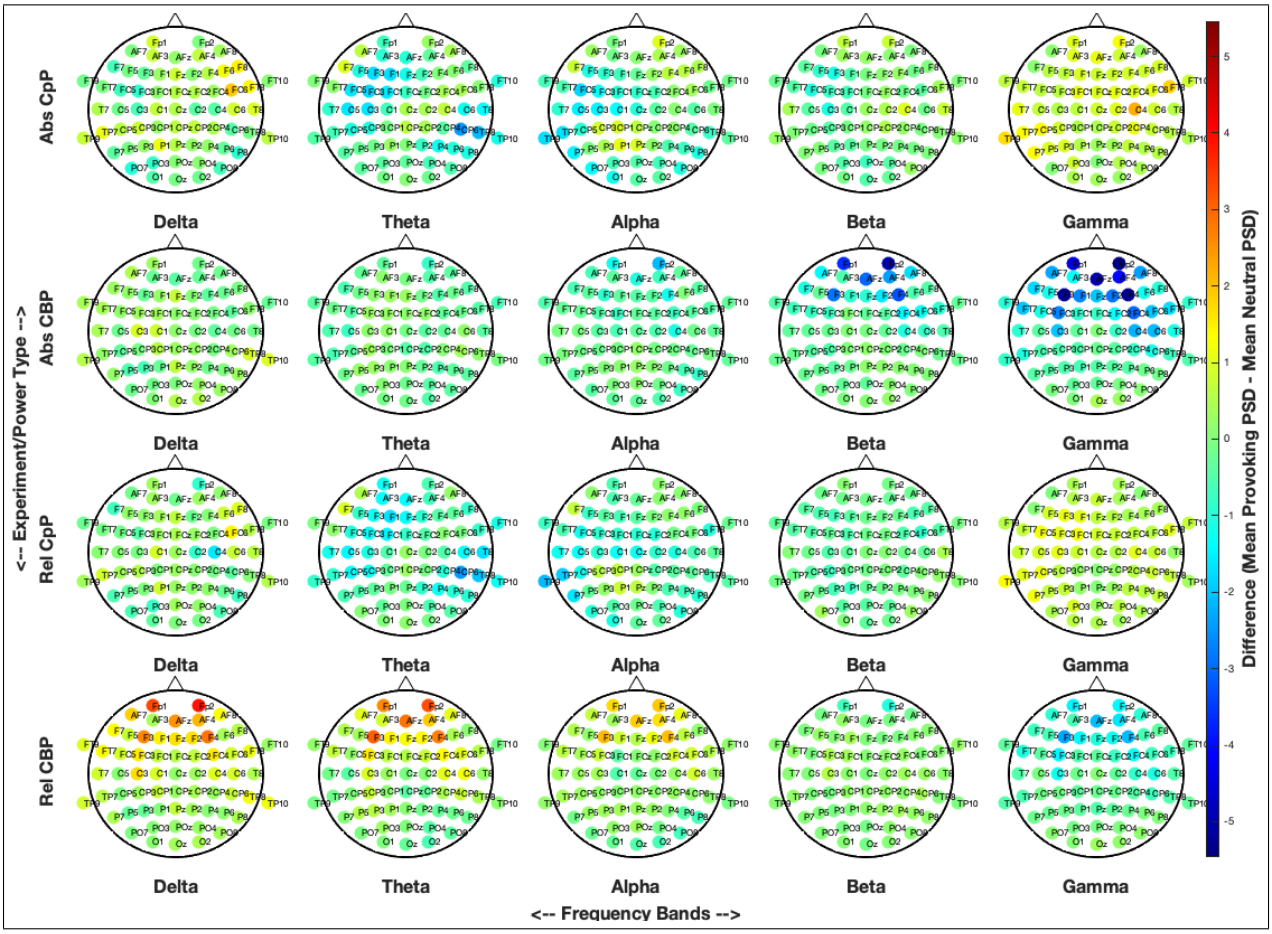

Figure 18: Direct State Comparison Topographic Visualization: Provoked vs Neutral. Blue indicates PSD decreases during provocation, Red indicates PSD increases during provocation, Green indicates no change.

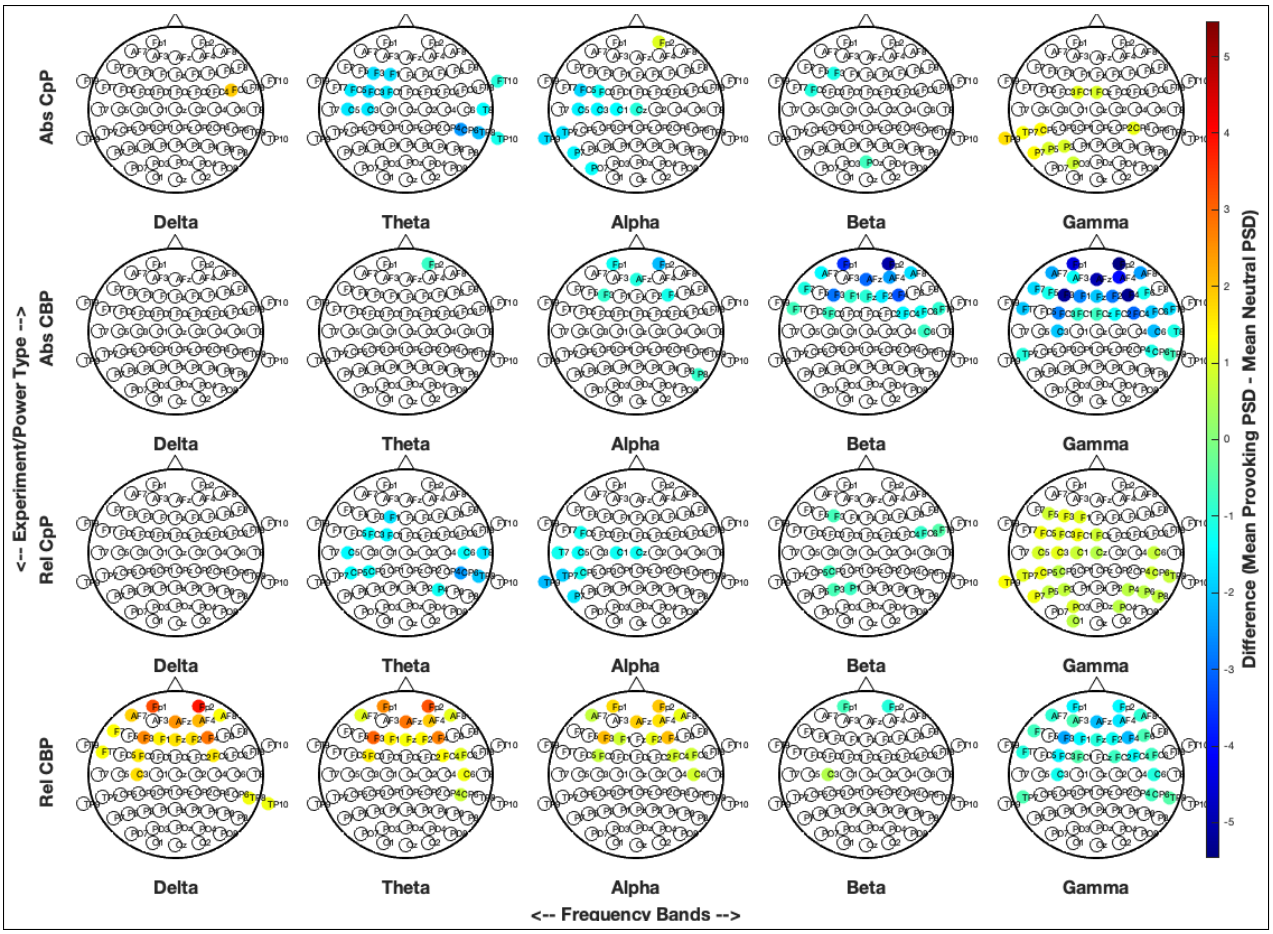

Figure 19: Direct State Comparison Topographic Visualization: Provoked vs Neutral. Blue indicates PSD decreases during provocation, Red indicates PSD increases during provocation, Green indicates no change. Channels where P > 0.05 are not colored in.

nificance into account. As the data are distributed across several epochs, an unpaired 2 sample t-test can indicate which channel/frequency/task combinations are more likely to be significantly different between states, and which are more likely to differ from random noise alone. Figure 19 re-visualizes the data using a significance threshold of 0.05: all combinations with p-values above this threshold are left uncolored.

This narrows the results down even further; however, with 1,280 combinations to choose from, false positives are still bound to occur even if no real difference between states truly exists. This is called the Multiple Comparison Problem and can be accounted for using a statistical technique called positive False Discovery Rate[48] (pFDR) correction, which considers the distribution of p-values from a given dataset (in this case, 320 p-values from a specific task and power type) to

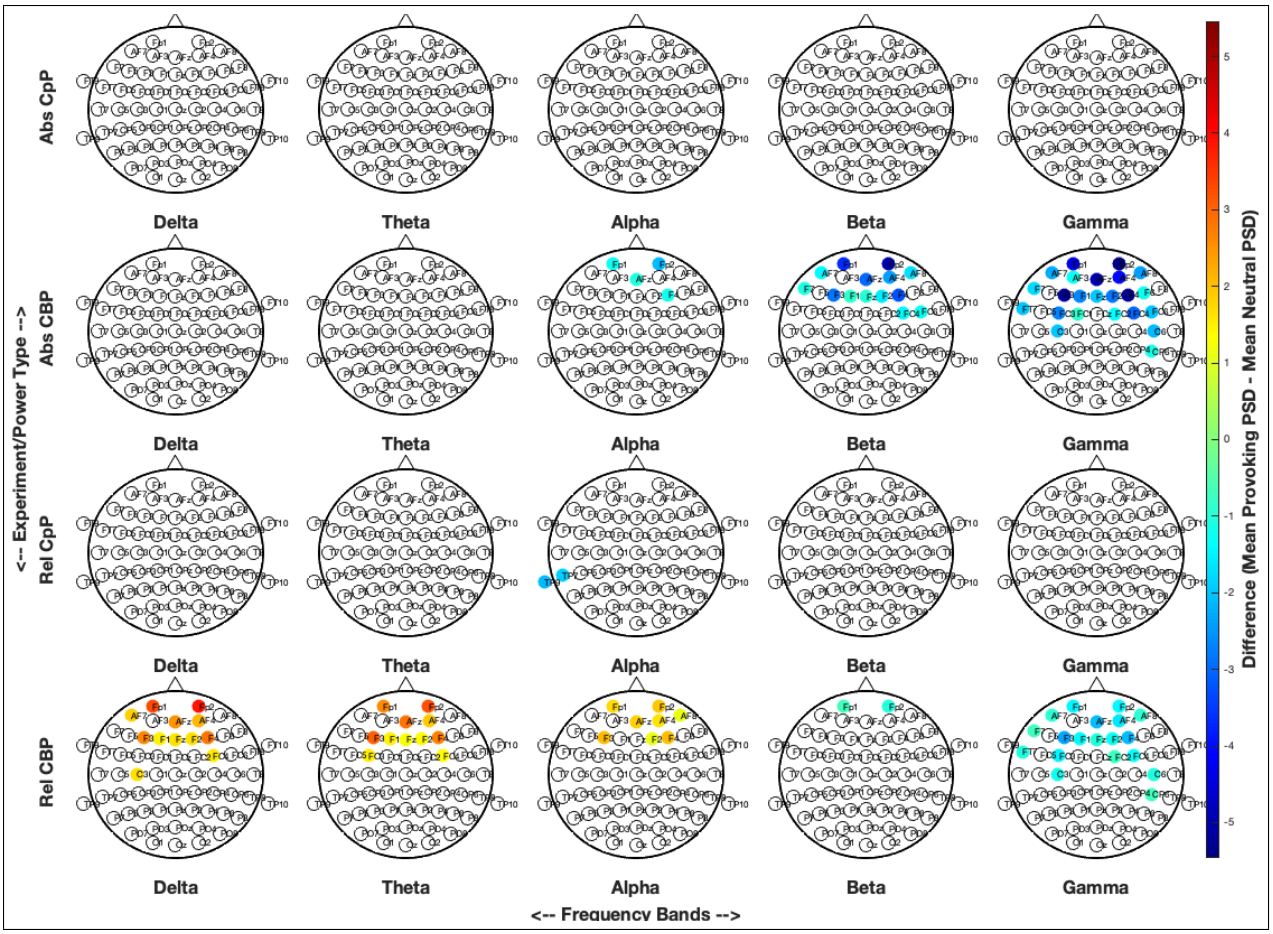

Figure 20: Direct State Comparison Topographic Visualization: Provoked vs Neutral. Blue indicates PSD decreases during provocation, Red indicates PSD increases during provocation, Green indicates no change. Channels where Q > 0.05 are not colored in.

generate an adjusted p-value called the q-value. These q-values represent the expected proportion of false positives among all combinations as or more significant (as defined by their p-value) than the given combination, as comparisons of non-correlated datasets are more likely to result in a flat distribution of p-values, while comparisons of correlated datasets are more likely to result in p-value distributions that are biased towards the lower extreme. Thus, a q-value threshold of 0.05 yields an expected 5% False Discovery Rate among deemed-significant combinations. Figure 20 visualizes the Direct State Comparison Topography again, this time only plotting combinations with q-values less than 0.05.

Finally, as behavioral analysis indicated that the participant was partially provoked during the CBP control trial, and as it is possible the participant was in a state of constant provocation during

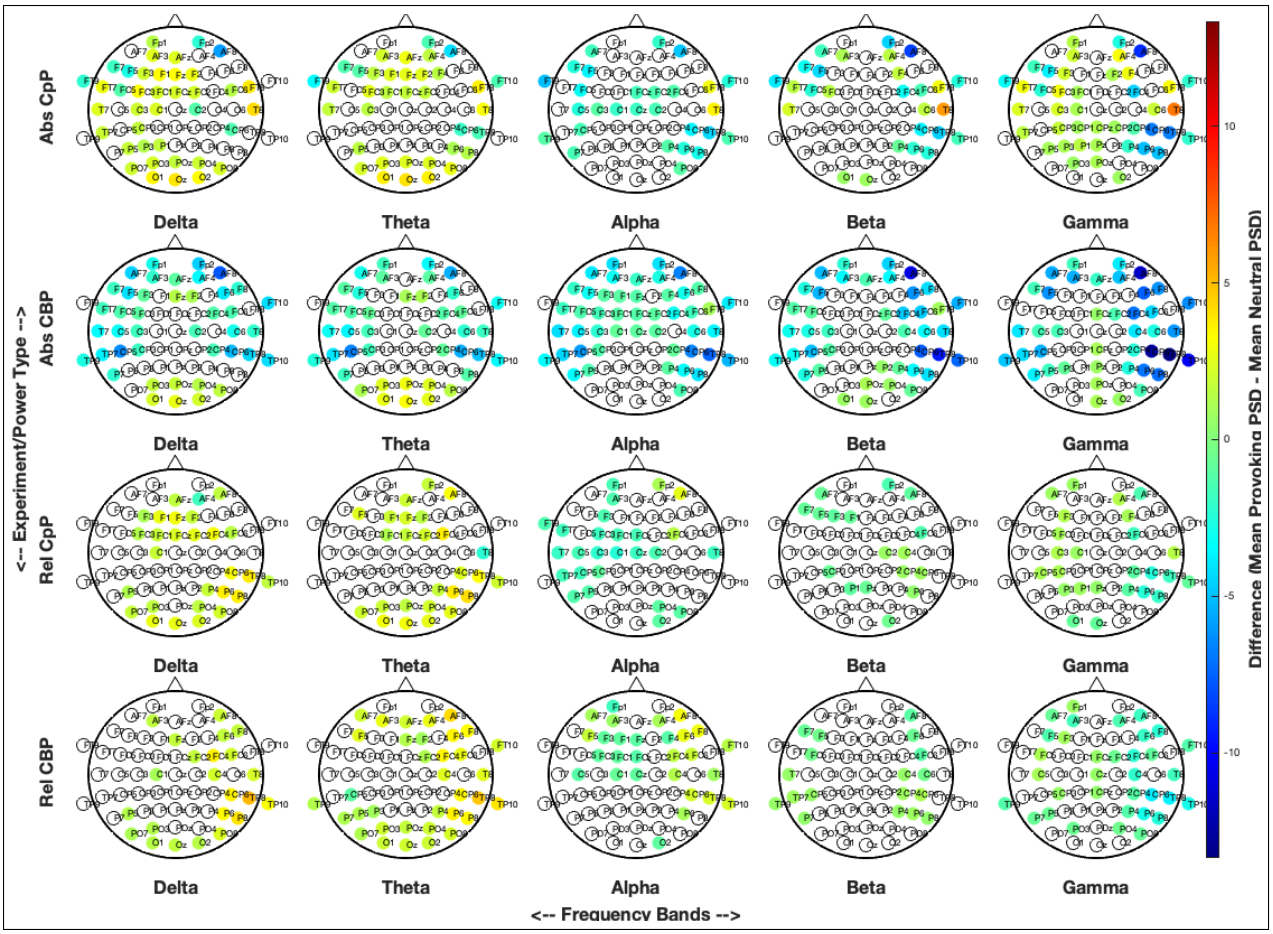

Figure 21: Direct State Comparison Topographic Visualization: Provoked vs Resting. Blue indicates PSD decreases during provocation, Red indicates PSD increases during provocation, Green indicates no change. Channels where Q > 0.05 are not colored in.

the CpP task, it is worthwhile to see if differences between the provoked and neutral state are preserved when comparing the provoked state to epochs (n=35) generated from resting-state data during which the participant was staring at a blank screen without moving. Mean PSD difference between provoked and resting state are visualized in Figure 21, again only plotting combinations where Q <= 0.05.

Visually certain features seems to be preserved, such as decreased absolute frontal Beta and Gamma during CBP, which logically corresponds to increased relative frontal power in the remaining signals (Delta, Theta, and Alpha). However, preserved vs resting returns far more combinations with significant differences between states. This is to be expected, as while the only predicted difference between provoking and neutral state is the immediate level of OCD provocation, provoking

vs resting state should additionally reflect the difference evoked by performing a task vs resting, anticipating a threat vs resting, or having recently been provoked vs resting.

Power Spectral Density: SUDS Correlation

SUDS Correlation uses the same set of epochs (Table 4) and calculated PSDs as Direct State Comparison; however, rather than finding the difference between states, this analysis seeks to find a correlation between PSD and increasing SUDS. Therefore, PSDs can be plotted against SUDS to visually look for correlation, as seen in in Figure 22.

Task	Epochs
CpP	34
CBP	89

Table 4: SUDS Correlation: Epochs per Task

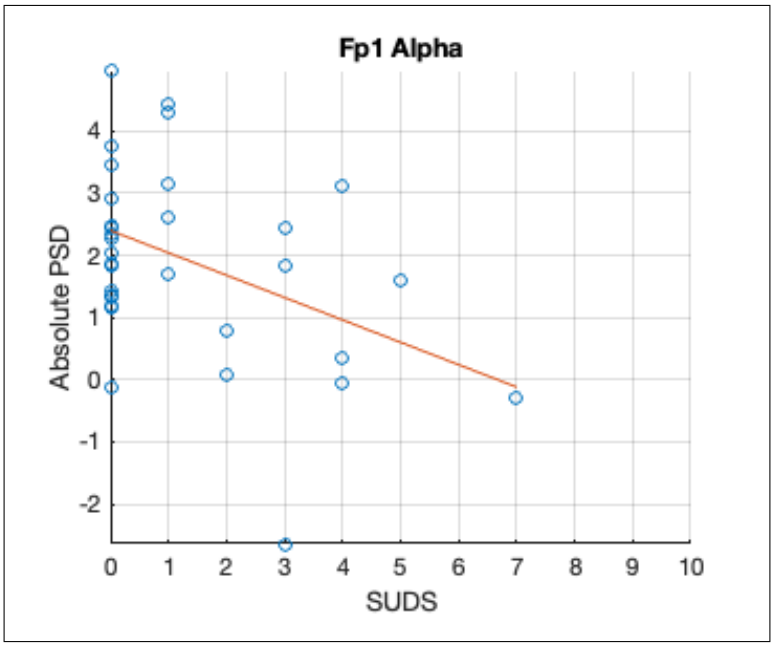

Figure 22: SUDS Correlation: Channel FP1 Abs Alpha During CpP. Absolute PSD units in dB. Linear Regression Plotted in Red.

Strength of SUDS Correlation is quantified by finding the Pearson Correlation[49] between SUDS and PSD, with 0 representing no correlation, values closer to 0 representing a weak linear correlation, values closer to 1 representing a strong positive linear correlation, and values closer to -1

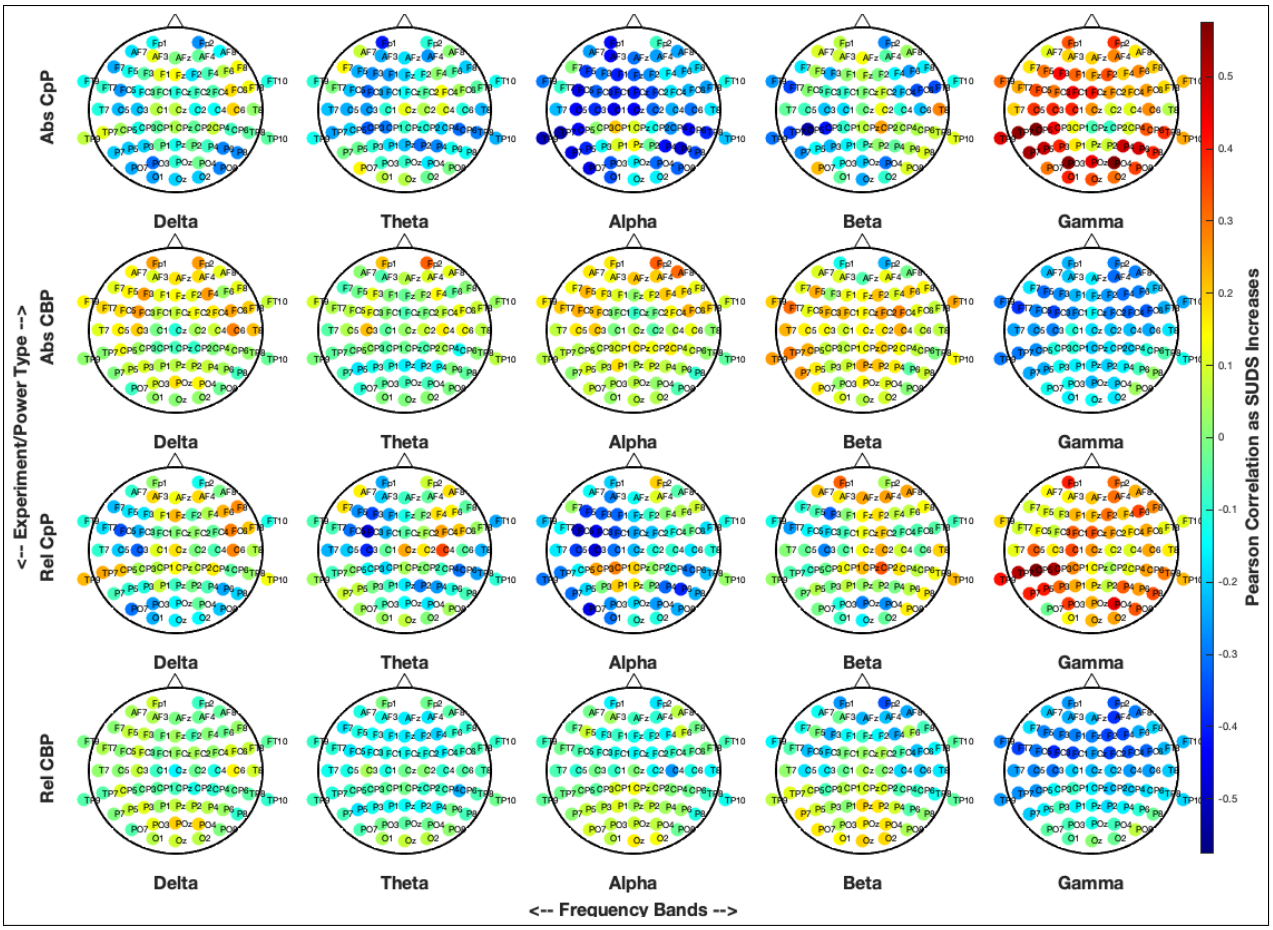

Figure 23: SUDS Correlation Topographic Visualization. Blue indicates PSD decreases with increased provocation, Red indicates PSD increases with increased provocation, Green indicates no change.

representing a strong negative linear correlation. Similar to Direct State Comparison, these values can be topographically displayed (Figure 23) to aid visual analysis. A two-tailed significance test can then be used to generate a t-distribution and corresponding p-values as visualized in Figure 24. Finally, pFDR can further increase confidence in the results by generating adjusted q-values, as visualized in Figure 25. Notably, the value of the Pearson Correlation does not correspond to the slope of correlation, only strength and direction, meaning that these values, unlike Direct State Comparison, merely indicate the tightness of correlation rather than indicating intensity.

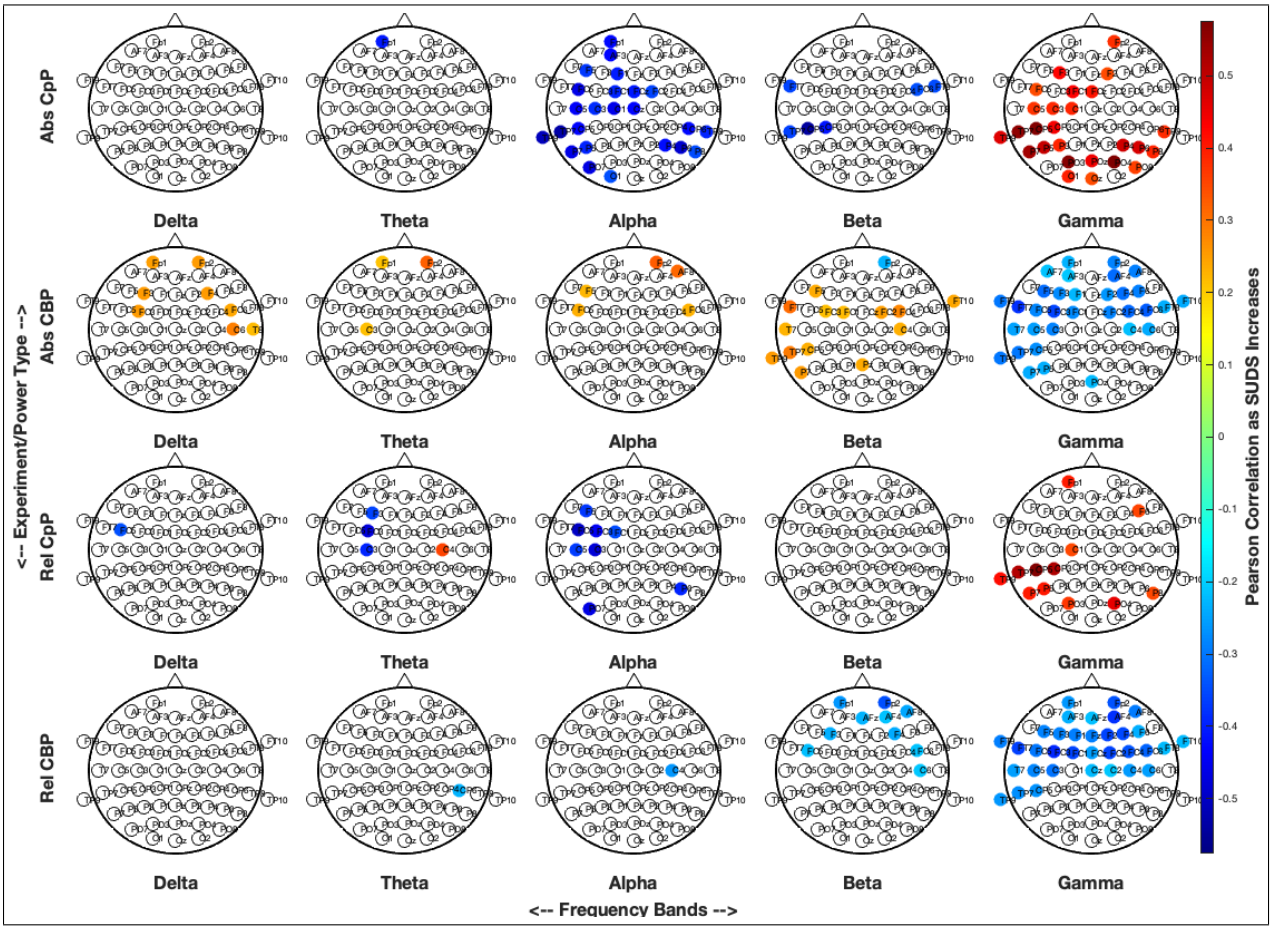

Figure 24: SUDS Correlation Topographic Visualization. Blue indicates PSD decreases with increased provocation, Red indicates PSD increases with increased provocation, Green indicates no change. Channels where P > 0.05 are not colored in.

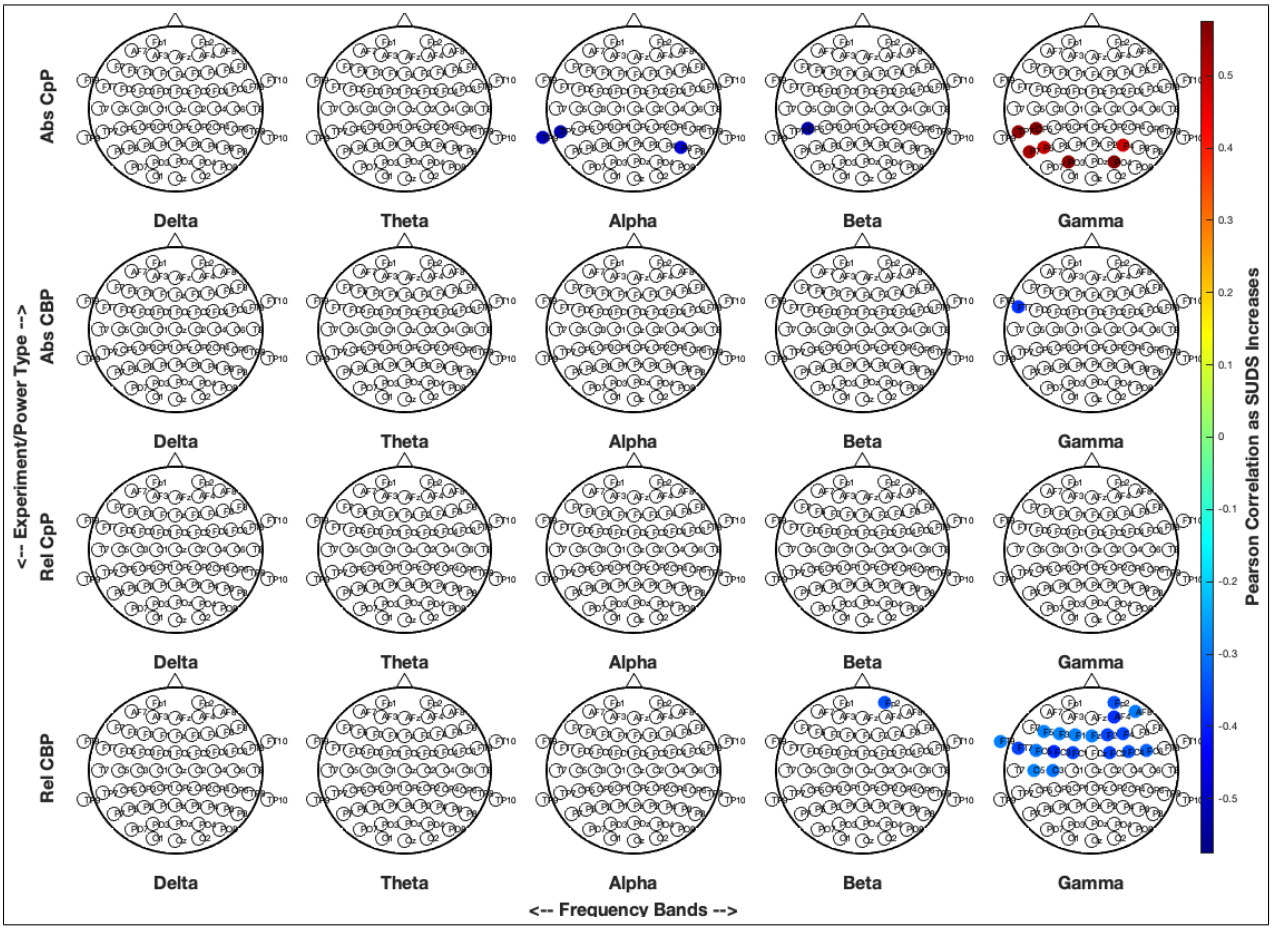

Figure 25: SUDS Correlation Topographic Visualization. Blue indicates PSD decreases with increased provocation, Red indicates PSD increases with increased provocation, Green indicates no change. Channels where Q > 0.05 are not colored in.

Chapter 6: Initial Conclusion, Task Validation, and Future Work

PROVOC Case Study Results and Future EEG Analysis

Considering only significant (Q <= 0.05) channel/task/power combinations, initial findings from BH_301 in project PROVOC suggest a decrease in frontal Gamma power during provocation. This comes from trends visible within clusters of blue (i.e. decreased/decreasing) frontal channels in Figures 22 and 25; the former relying on differentiating brain activity by researcher-determined trial type and the latter relying on correlating brain activity with participant-determined SUDS rating.

These results are intentionally broad at this level of analysis. While the implicated frontal channels are anatomically close to some OCD-related brain areas like OFC and ACC, it would be incorrect to conclude that decreased Gamma power in those brain areas are probably responsible for this result, as several other brain areas, such as DLPFC, are similarly involved in contributing to the same signal recorded at the implicated-scalp electrodes. However, should 'general' decreased frontal Gamma prove to be a trend in future participants, aDBS could potentially incorporate frontal ECoG into its closed-loop algorithm to better detect OC states.

Nonetheless, with the initial qEEG pipeline constructed and initial differences in PSD visible, future EEG analysis can expand towards identifying neuro-anatomically specific results, which will likely be necessary if closed-loop aDBS algorithms are to benefit from this research. Source localization, a signal processing methodology growing in popularity within the biomedical engineering community, could be particularly useful in this respect. Source localization aims to overcome EEG's poor spatial resolution by using temporal differences in EEG signal called dipoles to solve the inverse problem of predicting the cortical locations from which the components of a signal are originally generated.[50] However, accurate skull thickness maps are highly recommended to improve the accuracy of this analysis, meaning that the project's protocol would ideally be adjusted to include MRI imaging, which is unlikely at this phase.

Task Validation

At this stage in project PROVOC's existence, validating the task structure is much more important than drawing neuroanatomical conclusions from one participant's data. Towards that end, meaningful conclusions can still be drawn from the existing analysis, not towards discovering biomarkers of OCD, but towards validating the project's structure itself.

As briefly discussed in Chapter 4, the first major finding and potential issue is that of unintentional provocation. In this case, the participant erroneously suspected that the control object during Conveyor Belt PROVOC might be contaminated. As pathological doubt is a core trait of OCD, questioning whether or not a foreign object is contaminated is not surprising, and as participants are told during the consenting process that their symptoms will be provoked, it is entirely possible that unintentional provocation by the control object will happen in subsequent participants. However, a protocol modification to verbally inform the participant that the (designated control) object is truly neutral before the task begins might assuage some of this worry, making the trial a better representation of the neutral state for future Direct State Comparisons.

Furthermore, visual analysis of Figure 18 and especially Figure 23 indicate disagreement between the CpP and CBP tasks, particularly in the Gamma frequency band. The reason for this disagreement is not clear though the participant's facial tics, which would cause EMG noise heavily overlapping with even the 30-45 Hz adjusted Gamma range, could be to blame. For future participants, better screening to disqualify participants with facial tics might be necessary to make Gamma more consistent. However, outside of Gamma, the CpP task returned far fewer significant results than CBP. This could be because the participant reacted more strongly to seeing a provoking stimulus in-person despite the max SUDS rating being 7 in CpP and only 6 in CBP. But, given the highly subjective nature of SUDS ratings, it is likely unwise to compare them between tasks. Furthermore, the CpP task had about 1/3rd as many usable epochs as CBP. This likely reduced CpP's statistical power, resulting in fewer significant results.

Finally, more work needs to be done to ensure ECG and GSR recordings are properly collected

during the in-person visit. This will likely require choosing alternative locations where ECG leads will be less affected by sweat, such as by moving them from the chest to the wrists, where all of BH_301's usable ECG data was recorded. GSR on the other hand has been inconsistently collected even in practice visits, potentially necessitating its removal from the protocol entirely.

Yet, despite these minor shortcomings, the results of the first participant to complete an in-person visit for project PROVOC are promising. SUDS ratings indicate that with a few exceptions, the tasks are doing what they were meant to do, and the presence of significantly different/correlated channels, even if only from the CBP task, indicate that the project's foundational goal of evoking detectably different brain states using the provocation of OCD symptoms has been achieved. With this validation complete and the basic analysis pipeline constructed, project PROVOC can continue recruiting OCD participants to see if these results are consistent across subjects and recruit healthy control and specific phobia participants to expand analysis even further. Ideally, that expansion will achieve this research's primary goal: gaining an sufficient understanding of OCD brain activity to improve closed-loop aDBS, which, if successful, could improve the lives of those suffering from the most intractable, intense forms of OCD.

References

[1] R. C. Kessler, P. Berglund, O. Demler, R. Jin, K. R. Merikangas, and E. E. Walters, "Lifetime prevalence and age-of-onset distributions of DSM-IV disorders in the National Comorbidity Survey Replication.," *Archives of general psychiatry*, vol. 62, pp. 593–602, 6 2005.

[2] A. M. Ruscio, D. J. Stein, W. T. Chiu, and R. C. Kessler, "The epidemiology of obsessive-compulsive disorder in the National Comorbidity Survey Replication," *Molecular Psychiatry*, vol. 15, pp. 53–63, 1 2010.

[3] D. J. Stein, D. L. C. Costa, C. Lochner, E. C. Miguel, Y. C. J. Reddy, R. G. Shavitt, O. A. van den Heuvel, and H. B. Simpson, "Obsessive-compulsive disorder.," *Nature reviews. Disease primers*, vol. 5, p. 52, 8 2019.

[4] American Psychatric Association, "Diagnostic and Statistical Manual of Mental Disorders (5th ed.)," tech. rep., 2013.

[5] V. Starcevic, D. Berle, V. Brakoulias, P. Sammut, K. Moses, D. Milicevic, and A. Hannan, "Functions of Compulsions in Obsessive–Compulsive Disorder," *Australian \& New Zealand Journal of Psychiatry*, vol. 45, no. 6, pp. 449–457, 2011.

[6] M. E. Coles, A. S. Hart, and C. A. Schofield, "Initial data characterizing the progression from obsessions and compulsions to full-blown obsessive compulsive disorder," *Cognitive Therapy and Research*, vol. 36, pp. 685–693, 12 2012.

[7] G. I. Van Schalkwyk, I. P. Bhalla, M. Griepp, B. Kelmendi, L. Davidson, and C. Pittenger, "Toward understanding the heterogeneity in obsessive-compulsive disorder: Evidence from narratives in adult patients.," *The Australian and New Zealand journal of psychiatry*, vol. 50, pp. 74–81, 1 2016.

[8] N. Attiullah, J. L. Eisen, and S. A. Rasmussen, "CLINICAL FEATURES OF OBSESSIVE-COMPULSIVE DISORDER," *Psychiatric Clinics of North America*, vol. 23, no. 3, pp. 469–491, 2000.

[9] R. T. LeBeau, D. Glenn, B. Liao, H. U. Wittchen, K. Beesdo-Baum, T. Ollendick, and M. G. Craske, "Specific phobia: A review of DSM-IV specific phobia and preliminary recommendations for DSM-V," 2 2010.

[10] W. K. Goodman, L. H. Price, S. A. Rasmussen, C. Mazure, R. L. Fleischmann, C. L. Hill, G. R. Heninger, and D. S. Charney, "The Yale-Brown Obsessive Compulsive Scale. I. Development, use, and reliability.," *Archives of general psychiatry*, vol. 46, pp. 1006–1011, 11 1989.

[11] A. Pinto, B. D. Greenberg, M. A. Grados, O. J. r. Bienvenu, J. F. Samuels, D. L. Murphy, G. Hasler, R. L. Stout, S. L. Rauch, Y. Y. Shugart, D. L. Pauls, J. A. Knowles, A. J. Fyer, J. T. McCracken, J. Piacentini, Y. Wang, V. L. Willour, B. Cullen, K.-Y. Liang, R. Hoehn-Saric, M. A. Riddle, S. A. Rasmussen, and G. Nestadt, "Further development of YBOCS dimensions in the OCD Collaborative Genetics study: symptoms vs. categories.," *Psychiatry research*, vol. 160, pp. 83–93, 7 2008.

[12] K. E. Burdick, D. G. Robinson, A. K. Malhotra, and P. R. Szeszko, "Neurocognitive profile analysis in obsessive-compulsive disorder," *Journal of the International Neuropsychological Society*, vol. 14, no. 4, pp. 640–645, 2008.

[13] T. Nakao, K. Okada, and S. Kanba, "Neurobiological model of obsessive–compulsive disorder: Evidence from recent neuropsychological and neuroimaging findings," *Psychiatry and Clinical Neurosciences*, vol. 68, no. 8, pp. 587–605, 2014.

[14] S. Saxena and S. L. Rauch, "FUNCTIONAL NEUROIMAGING AND THE NEUROANATOMY OF OBSESSIVE-COMPULSIVE DISORDER," *Psychiatric Clinics of North America*, vol. 23, no. 3, pp. 563–586, 2000.

[15] T. V. Maia, R. E. Cooney, and B. S. Peterson, "The neural bases of obsessive - Compulsive disorder in children and adults," 2008.

[16] J. T. Ting and G. Feng, "Neurobiology of obsessive-compulsive disorder: Insights into neural circuitry dysfunction through mouse genetics," 12 2011.

[17] M. L. Berthier, J. Kulisevsky, A. Gironell, and J. A. Heras, "Obsessive-compulsive disorder associated with brain lesions: Clinical phenomenology, cognitive function, and anatomic correlates," tech. rep., 1996.

[18] E. Burguière, P. Monteiro, L. Mallet, G. Feng, and A. M. Graybiel, "Striatal circuits, habits, and implications for obsessive-compulsive disorder," 1 2015.

[19] P. Fettes, L. Schulze, and J. Downar, "Cortico-striatal-thalamic loop circuits of the orbitofrontal cortex: Promising therapeutic targets in psychiatric illness," 4 2017.

[20] R. L. Albin, A. B. Young, and J. B. Penney, "The functional anatomy of basal ganglia disorders," tech. rep., 1989.

[21] B. D. Greenberg, S. L. Rauch, and S. N. Haber, "Invasive circuitry-based neurotherapeutics: Stereotactic ablation and deep brain stimulation for OCD," 1 2010.

[22] P. Blomstedt, R. L. Sjöberg, M. Hansson, O. Bodlund, and M. I. Hariz, "Deep brain stimulation in the treatment of obsessive-compulsive disorder," 12 2013.

[23] P. Alonso, D. Cuadras, L. Gabriëls, D. Denys, W. Goodman, B. D. Greenberg, F. Jimenez-Ponce, J. Kuhn, D. Lenartz, L. Mallet, B. Nuttin, E. Real, C. Segalas, R. Schuurman, S. T. Du Montcel, and J. M. Menchon, "Deep brain stimulation for obsessive-compulsive disorder: A meta-analysis of treatment outcome and predictors of response," *PLoS ONE*, vol. 10, 7 2015.

[24] P. Alonso, J. M. Menchon, J. Pifarre, D. Mataix-Cols, L. Torres, P. Salgado, and J. Vallejo, "Long-term follow-up and predictors of clinical outcome in obsessive-compulsive patients

treated with serotonin reuptake inhibitors and behavioral therapy.," *The Journal of clinical psychiatry*, vol. 62, pp. 535–540, 7 2001.

[25] J. L. Eisen, W. K. Goodman, M. B. Keller, M. G. Warshaw, L. M. DeMarco, D. D. Luce, and S. A. Rasmussen, "Patterns of remission and relapse in obsessive-compulsive disorder: a 2-year prospective study.," *The Journal of clinical psychiatry*, vol. 60, pp. 346–51, 5 1999.

[26] K. A. Lapidus, E. R. Stern, H. A. Berlin, and W. K. Goodman, "Neuromodulation for Obsessive-Compulsive Disorder," 2014.

[27] E. B. Montgomery and J. T. Gale, "Mechanisms of action of deep brain stimulation (DBS)," 2008.

[28] T. M. Herrington, J. J. Cheng, and E. N. Eskandar, "Mechanisms of deep brain stimulation," *J Neurophysiol*, vol. 115, pp. 19–38, 2016.

[29] N. R. Provenza, E. R. Matteson, A. B. Allawala, A. Barrios-Anderson, S. A. Sheth, A. Viswanathan, E. McIngvale, E. A. Storch, M. J. Frank, N. C. R. McLaughlin, J. F. Cohn, W. K. Goodman, and D. A. Borton, "The Case for Adaptive Neuromodulation to Treat Severe Intractable Mental Disorders," *Frontiers in neuroscience*, vol. 13, p. 152, 2 2019.

[30] N. V. Thakor and S. Tong, "Advances in quantitative electroencephalogram analysis methods," *Annual Review of Biomedical Engineering*, vol. 6, pp. 453–495, 2004.

[31] H. R. Gupta, "Power Spectrum Estimation using Welch Method for various Window Techniques," vol. 2, no. 6, pp. 389–392, 2013.

[32] L. S. Prichep and E. R. John, "QEEG profiles of psychiatric disorders," *Brain Topography*, vol. 4, no. 4, pp. 249–257, 1992.

[33] L. Livint Popa, H. Dragos, C. Pantelemon, O. Verisezan Rosu, and S. Strilciuc, "The Role of Quantitative EEG in the Diagnosis of Neuropsychiatric Disorders," *Journal of medicine and life*, vol. 13, no. 1, pp. 8–15, 2020.

[34] J. J. Newson and T. C. Thiagarajan, "EEG Frequency Bands in Psychiatric Disorders: A Review of Resting State Studies," *Frontiers in Human Neuroscience*, vol. 12, no. January, pp. 1–24, 2019.

[35] Brain Products GmbH, "actiCHamp Plus (64 Channels)," 2019.

[36] Brain Products GmbH, "BrainVision Recorder (Version 2.2.0)," 2019.

[37] B. C. P.J. Lang, M.M. Bradley, "International affective picture system (IAPS): Affective ratings of pictures and instruction manual. Technical Report A-8.," 2008.

[38] E. A. Storch, S. A. Rasmussen, L. H. Price, M. J. Larson, T. K. Murphy, and W. K. Goodman, "Development and psychometric evaluation of the Yale–Brown Obsessive-Compulsive Scale—Second Edition.," 2010.

[39] E. B. Foa, J. D. Huppert, S. Leiberg, R. Langner, R. Kichic, G. Hajcak, and P. M. Salkovskis, "The Obsessive-Compulsive Inventory: Development and validation of a short version.," 2002.

[40] K. H. Sheehan and D. V. Sheehan, "Assessing treatment effects in clinical trials with the Discan metric of the Sheehan Disability Scale," *International Clinical Psychopharmacology*, vol. 23, no. 2, 2008.

[41] J. H. Siegle, A. C. López, Y. A. Patel, K. Abramov, S. Ohayon, and J. Voigts, "Open Ephys: An open-source, plugin-based platform for multichannel electrophysiology," *Journal of Neural Engineering*, vol. 14, no. 4, 2017.

[42] A. Delorme and S. Makeig, "EEGLAB: an open source toolbox for analysis of single-trial EEG dynamics," *Journal of Neuroscience Methods*, vol. 134, no. 1, pp. 9–21, 2004.

[43] T. R. Mullen, C. A. Kothe, Y. M. Chi, A. Ojeda, T. Kerth, S. Makeig, T. P. Jung, and G. Cauwenberghs, "Real-time neuroimaging and cognitive monitoring using wearable dry EEG," *IEEE Transactions on Biomedical Engineering*, vol. 62, no. 11, pp. 2553–2567, 2015.

[44] C. Y. Chang, S. H. Hsu, L. Pion-Tonachini, and T. P. Jung, "Evaluation of Artifact Subspace Reconstruction for Automatic Artifact Components Removal in Multi-Channel EEG Recordings," *IEEE Transactions on Biomedical Engineering*, vol. 67, no. 4, pp. 1114–1121, 2020.

[45] I. I. Christov, "Real time electrocardiogram QRS detection using combined adaptive threshold," *BioMedical Engineering Online*, vol. 3, pp. 1–9, 2004.

[46] F. Shaffer and J. P. Ginsberg, "An Overview of Heart Rate Variability Metrics and Norms," *Frontiers in Public Health*, vol. 5, no. September, pp. 1–17, 2017.

[47] R. Martinek, M. Ladrova, M. Sidikova, R. Jaros, K. Behbehani, R. Kahankova, and A. Kawala-Sterniuk, "Advanced bioelectrical signal processing methods: Past, present, and future approach—part iii: Other biosignals," *Sensors*, vol. 21, no. 18, pp. 1–32, 2021.

[48] J. D. Storey, "The positive false discovery rate: A Bayesian interpretation and the q-value," *Annals of Statistics*, vol. 31, no. 6, pp. 2013–2035, 2003.

[49] "Pearson's Correlation Coefficient," in *Encyclopedia of Public Health* (W. Kirch, ed.), pp. 1090–1091, Dordrecht: Springer Netherlands, 2008.

[50] C. M. Michel and D. Brunet, "EEG source imaging: A practical review of the analysis steps," *Frontiers in Neurology*, vol. 10, no. APR, 2019.

Appendix

Appendix A: Computer PROVOC Direct State Comparison Spectra

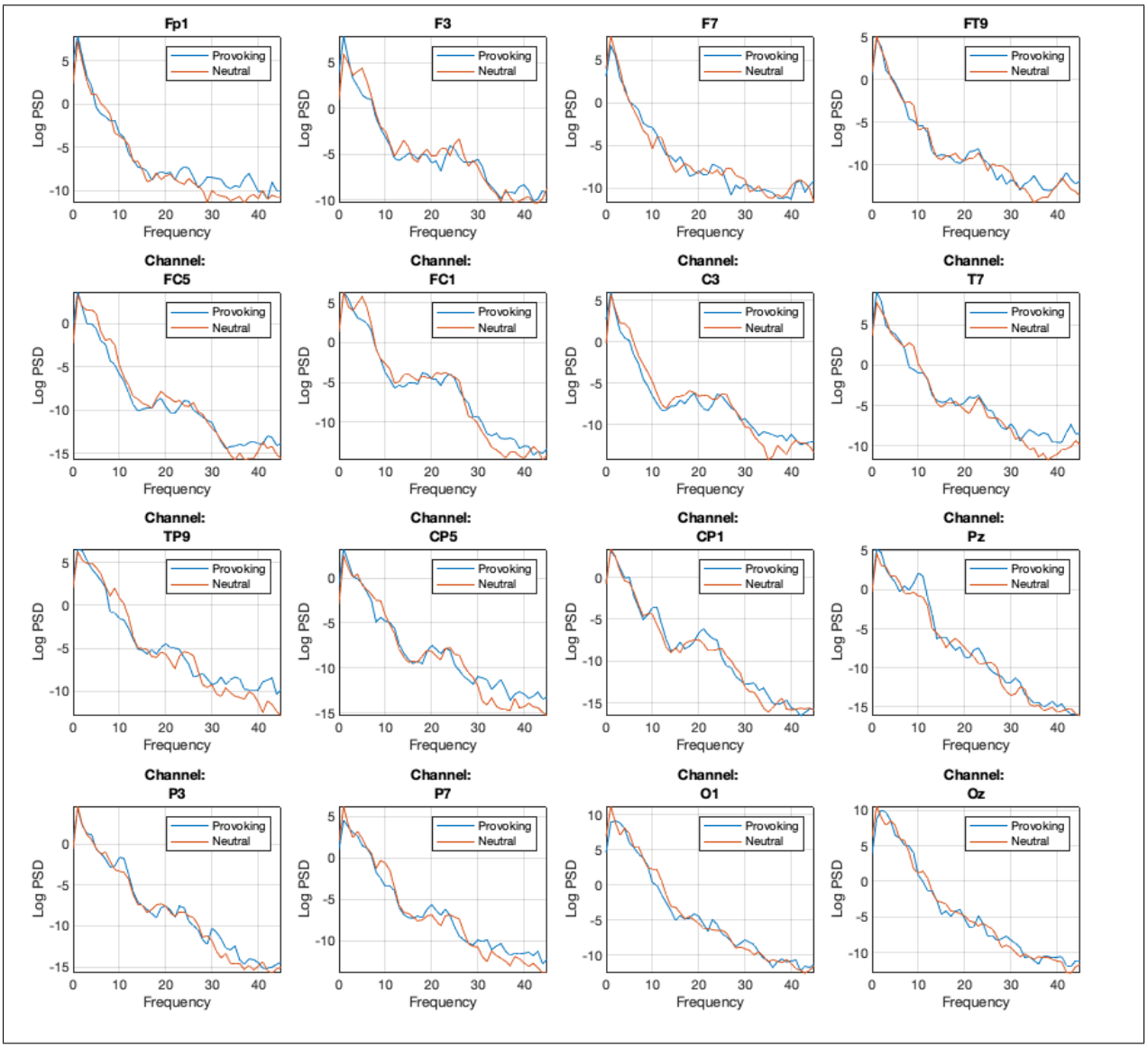

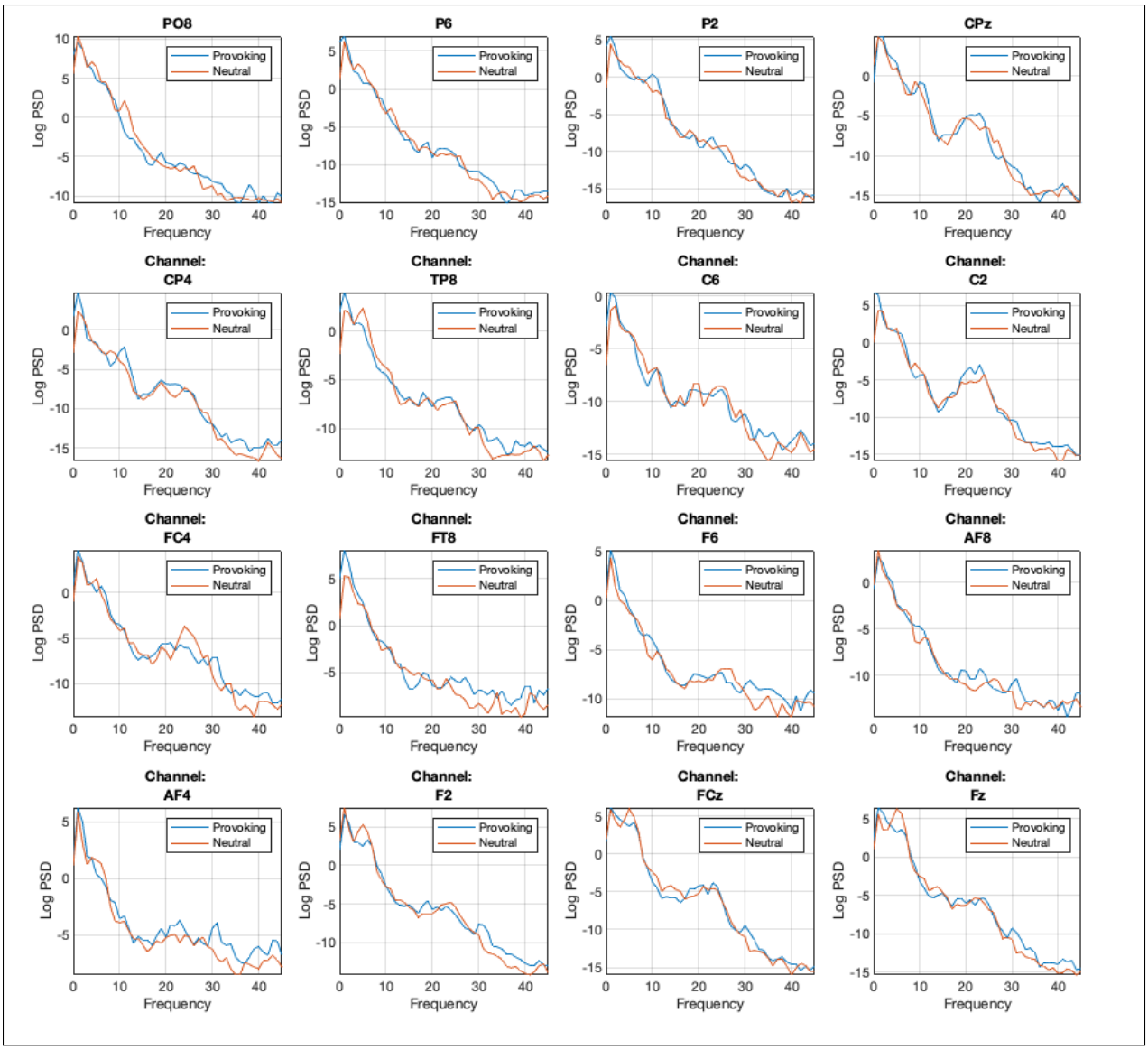
PO8
P6
P2
CPz
Channel: CP4
Channel: TP8
Channel: C6
Channel: C2
Channel: FC4
Channel: FT8
Channel: F6
Channel: AF8
Channel: AF4
Channel: F2
Channel: FCz
Channel: Fz
Provoking
Neutral
Log PSD
Frequency

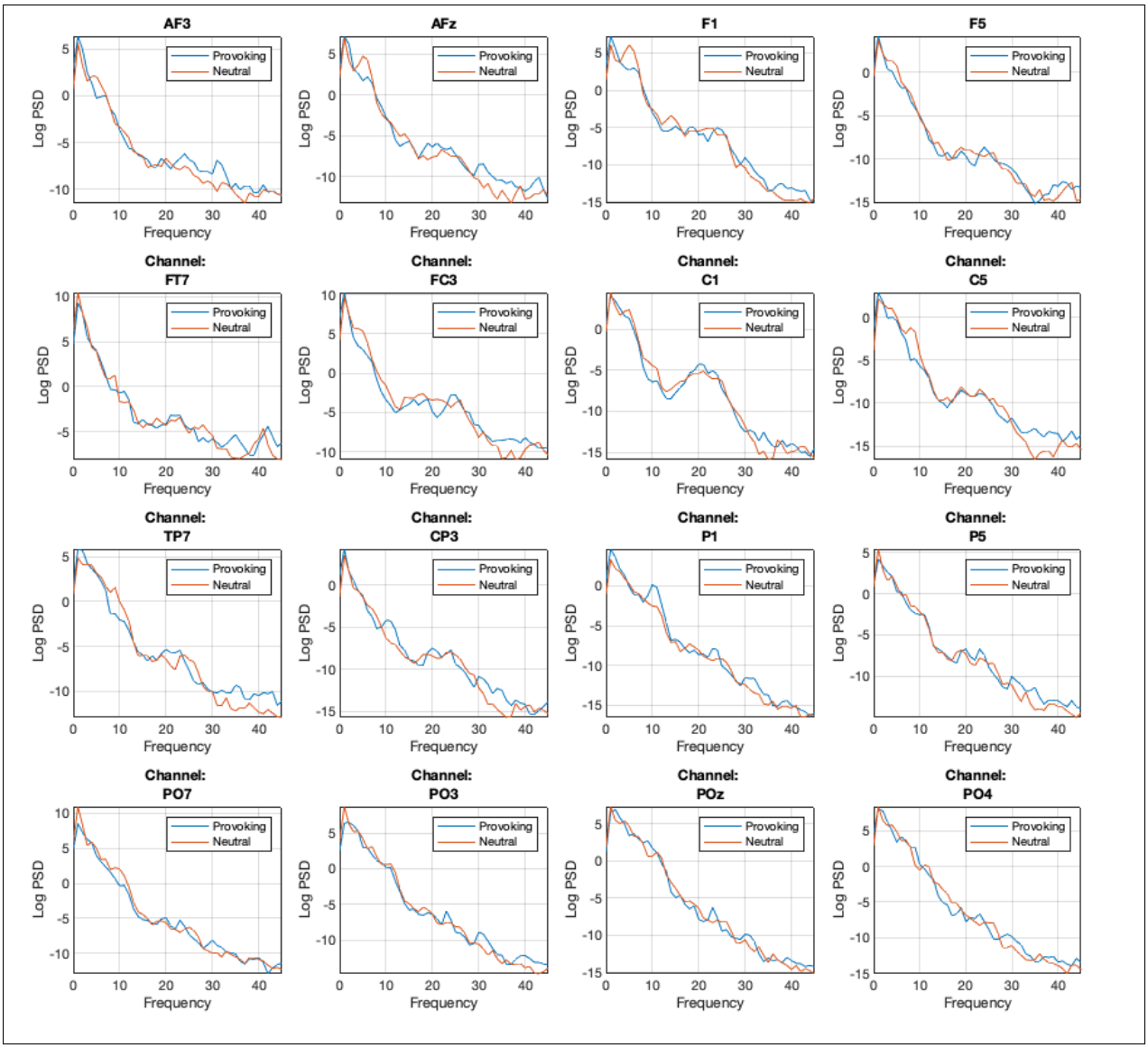
AF3
AFz
F1
F5
Channel: FT7
Channel: FC3
Channel: C1
Channel: C5
Channel: TP7
Channel: CP3
Channel: P1
Channel: P5
Channel: PO7
Channel: PO3
Channel: POz
Channel: PO4
Provoking
Neutral
Log PSD
Frequency

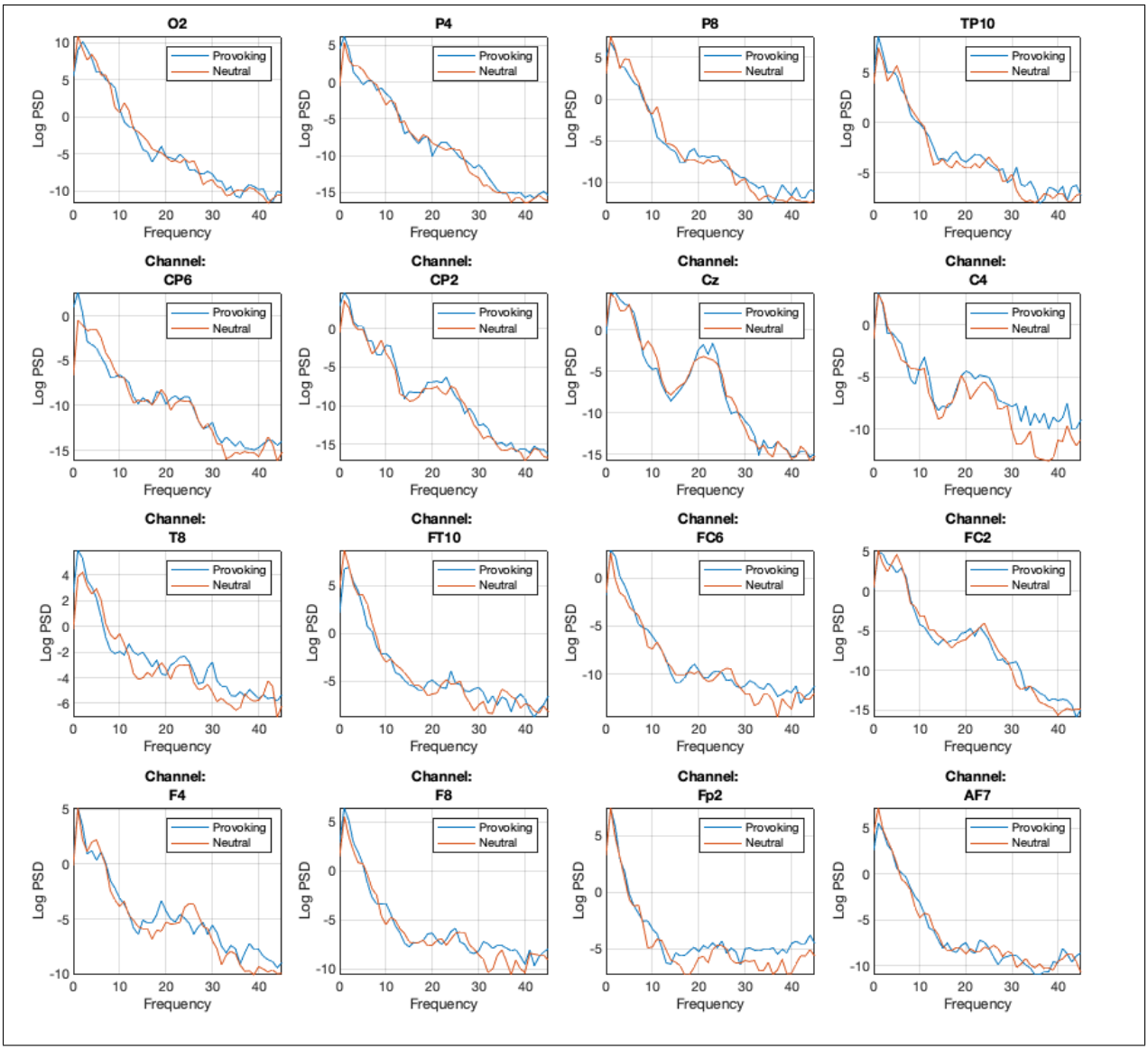
O2
P4
P8
TP10
Channel: CP6
Channel: CP2
Channel: Cz
Channel: C4
Channel: T8
Channel: FT10
Channel: FC6
Channel: FC2
Channel: F4
Channel: F8
Channel: Fp2
Channel: AF7
Provoking
Neutral
Log PSD
Frequency

Appendix B: Conveyor Belt PROVOC Direct State Comparison Spectra

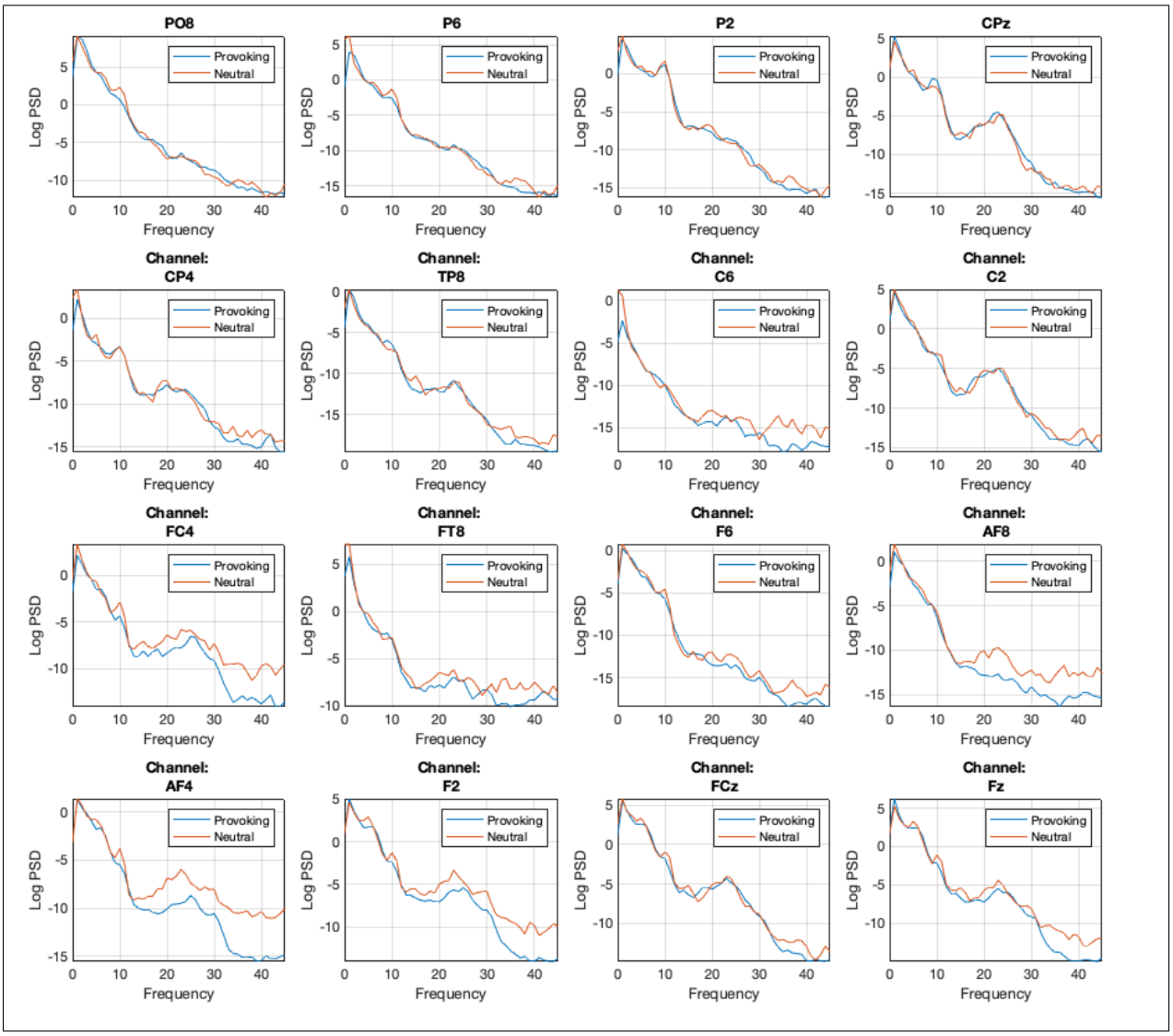

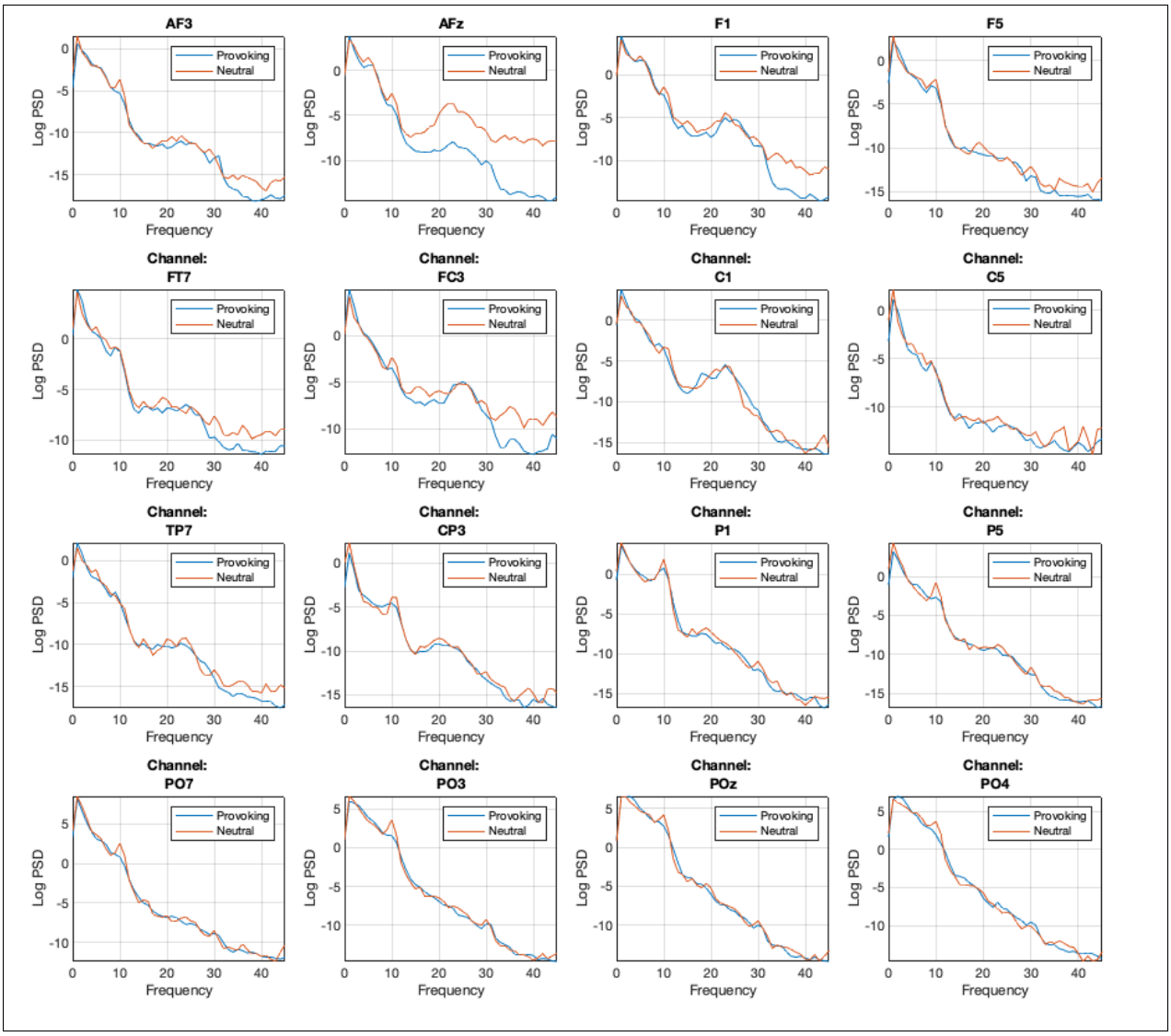
AF3
AFz
F1
F5
Channel: FT7
Channel: FC3
Channel: C1
Channel: C5
Channel: TP7
Channel: CP3
Channel: P1
Channel: P5
Channel: PO7
Channel: PO3
Channel: POz
Channel: PO4
Provoking
Neutral
Log PSD
Frequency

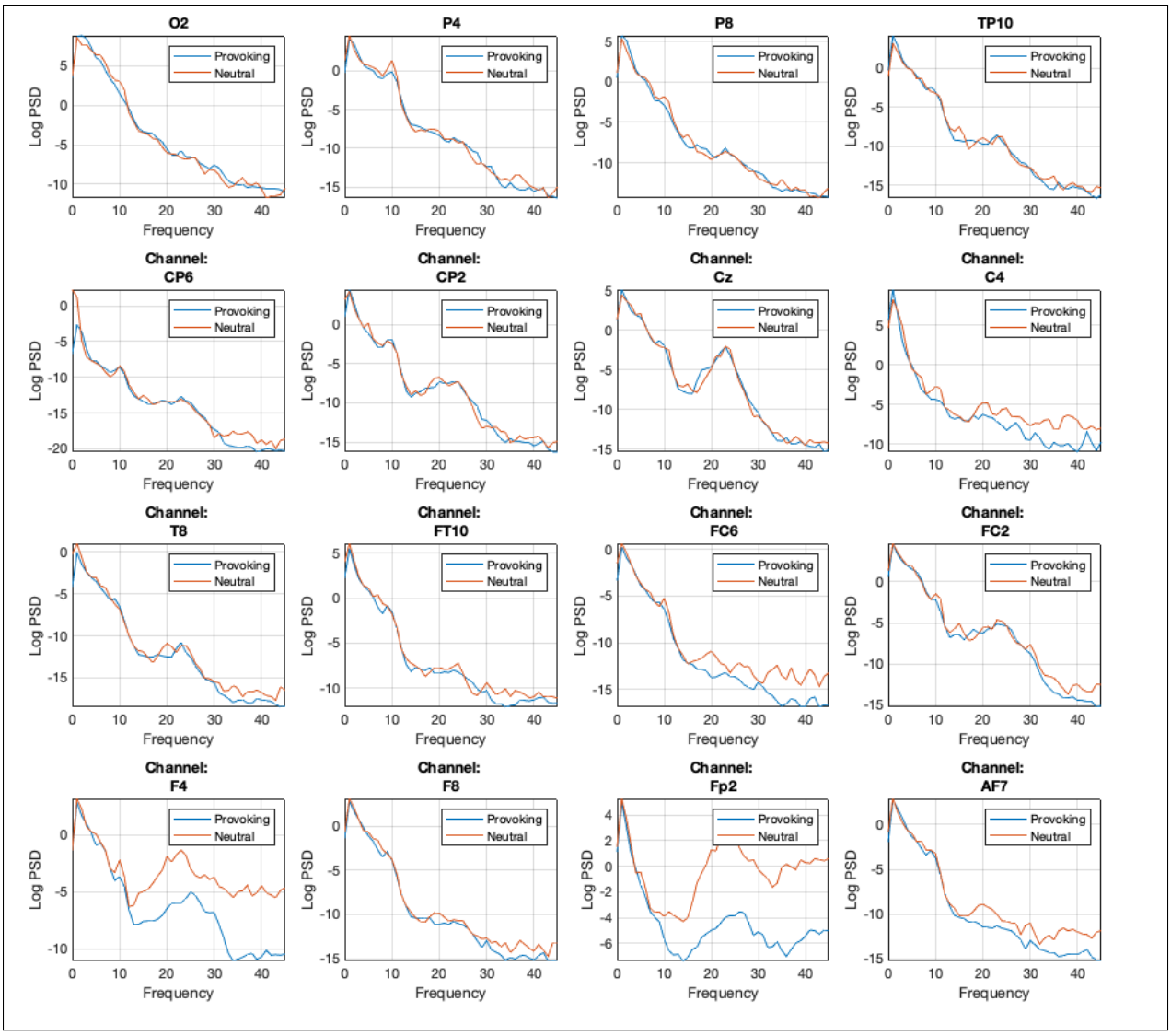
O2
P4
P8
TP10
Channel: CP6
Channel: CP2
Channel: Cz
Channel: C4
Channel: T8
Channel: FT10
Channel: FC6
Channel: FC2
Channel: F4
Channel: F8
Channel: Fp2
Channel: AF7
Provoking
Neutral
Log PSD
Frequency

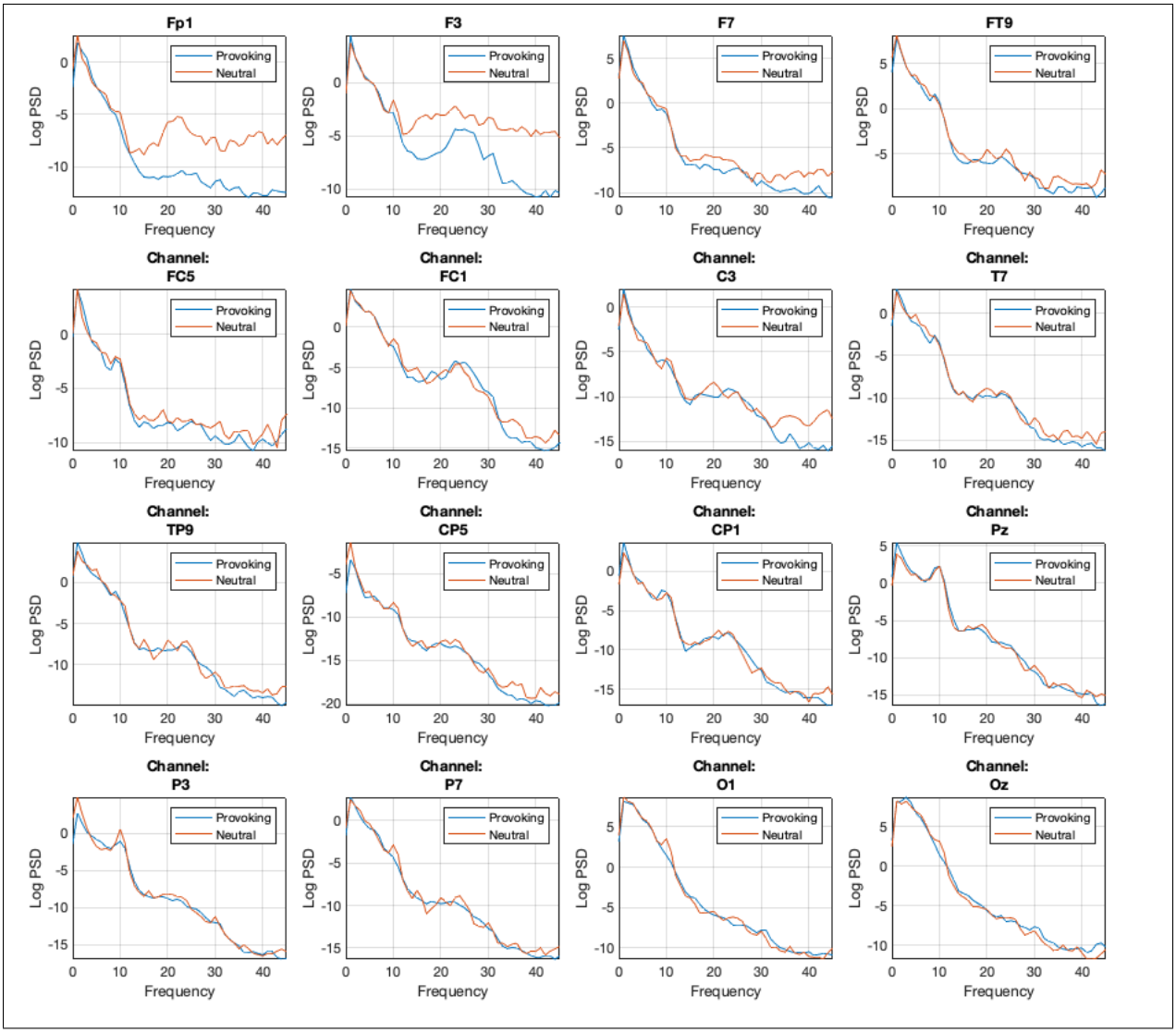
Fp1
F3
F7
FT9
Channel: FC5
Channel: FC1
Channel: C3
Channel: T7
Channel: TP9
Channel: CP5
Channel: CP1
Channel: Pz
Channel: P3
Channel: P7
Channel: O1
Channel: Oz
Provoking
Neutral
Log PSD
Frequency